Author's response to the reviews of *Surge Dynamics and lake outbursts of Kyagar Glacier, Karakoram*

Dear Editors and Reviewers,

Please find below our final response to the reviews from Martin Truffer and Christoph Mayer, followed by a marked up latexdiff version of the revised manuscript. The response to the reviews is structured in the following manner: reviewer's comment (bold text), author's response (plain text), and changes to manuscript (italic text). Note that the page, line and figure references in the response refer to the discussion paper rather than the new manuscript. There may be minor differences between the responses submitted to the discussion and the responses below, due to final editing.

Response to review from Martin Truffer

We would like to thank Martin Truffer for the insightful and positive review. It will undoubtedly help us improve a few points in the paper. We address each of his points and outline the corresponding changes to the manuscript.

This is a very well written and interesting paper documenting most of a surge cycle of Kyagar Glacier in the Karakoram. While it is known that this mountain range has surge-type glaciers, it remains very under-studied and this paper adds a wealth of information. The satellite data coverage is amazing and allows the deduction of both elevation changes and the velocity evolution during the lead-up two a two-phase surge. The paper is essentially free of errors and well-written and could basically be published as is. I have a few small comments that should be considered for final revision:

The PDD analysis is a bit of a side-line to this paper. I do like something like it, because the availability of melt water is an important part of the story. A few more details would help: 1) It is stated that PDD is calculated from hourly data. Are the hourly data used to calculate a daily average, or are these actually 'positive degree hours'?

The hourly air temperature measurements were used to create the equivalent of an average daily temperature by weighting the hourly measurements by the fraction of a day which they represent. We adjusted the text to make this clearer (p.11, l.14):

"Positive degree days (PDD) at the glacier terminus were calculated as a proxy for potential melting. Positive air temperature measurements were summed with each measurement weighted by the fraction of a day which it represented (Vaughan, 2006), such that one hourly measurement of 6°C would contribute 0.25 PDD. The hourly air temperature data from the station at Kyagar Glacier terminus were used (...)"

2) What is the meaning of calculating PDD at one point? If the weather station is at the terminus than a day with very low positive temperatures would presumably cause melt at the very lowest part of the glacier tongue only, whereas a high degree day would cause melting over large parts of the glacier. So this measure would be a very non-linear measure of melt?

Yes that's true, the calculated PDD is a value representing conditions at the terminus. The elevation range of the glacier and an estimated lapse rate can be used to make a short statement about the expected melting period over the majority of the glacier rather than just at the terminus. We will rephrase the PDD section in 4.3 Meteorological observations on p.19 to clarify the points raised:

"Temperatures remained below 0°C between mid-October and late April according to data from the meteorological station at the glacier terminus (at 4800 m a.s.l.). The warmest months, July and August, experienced average daily maximum temperatures of 4–7°C and monthly PDDs exceeding 150 at the glacier terminus. By taking into account the elevation of the glacier surface and a lapse rate of about -0.006°C m^{-1}, it can be inferred that over the whole glacier tongue, PDDs are positive between May and October, whilst over the bulk of the accumulation area (about 900 m above the terminus) melt potential was only significant from June to August. Evidence of high-altitude melt is seen in the TanDEM-X backscatter images from August 2015 (supplementary Figure 1). Annual PDDs at the glacier terminus were 647°C, 481°C, 552°C and 528°C in 2013, 2014, 2015 and 2016, respectively."

3) Does the PDD contribute more to this paper than simply a temperature graph?

We include the PDD analysis primarily as a way to present the temperature data. We believe it gives a better overview of the temporal distribution of melt potential than a temperature plot, because it provides annual or monthly values which can easily be compared.

Eisen et al. (J.Glac., 2005) discuss surge initiation by a hydraulic switch that depends very sensitively on basal stress (p. 404/405). This discussion seems very relevant to this paper as well, and I recommend consulting it.

Thanks for this suggestion. The discussion on the sensitivity of the drainage system to increased basal stress is a very relevant reference which we shall add to p.22, l.11:

"Given the potential sensitivity of the subglacial drainage efficiency to basal stress (Eisen et al., 2005) the conditions at the end of the quiescence phase could be expected to favour the switch to an inefficient drainage system."

Also after reading Eisen et al. (2005) we intend to add this additional text to the discussion p.23, l.17, as we find the difference in seasonality of initiation and termination between many Alaskan surges and Kyagar Glacier worth noting:

"It seems that the surge is well explained by the presence of an inefficient basal drainage system facilitating high subglacial water pressure, corresponding to the mechanism proposed by Kamb et al. (1985). However, the seasonality observed at Kyagar Glacier is different to the often cited winter initiation associated with closure of subglacial channels in the hydrological switch mechanism (Eisen et al. 2005, Kamb et al., 1985). In the case of Kyagar Glacier, development of an inefficient drainage system in winter does not necessarily facilitate increased subglacial water pressure until the beginning of the melt season, due a lack of liquid water in winter. Surge initiation in winter should not be considered a precondition of hydrologically controlled surging (see e.g., Jiskoot & Low, 2011)."

p.9, l.14/15: This is a detail, but what you're discussing is not really an error, is it? You're simply deriving the horizontal component of the velocity vector. The way you

describe it you would assume that the velocity vector is surface parallel.

True, it makes more sense to use the term 'velocity difference' rather than 'velocity error'. This will be corrected in the manuscript.

p.11, l.11: delete ',' (unless this involves sticking tongues into glaciers :))

The offending comma will be removed to avoid misunderstanding!

p.12, l.22: The speed-up is not really uniform over the glacier tongue: the gradient gets much larger. An interesting feature is an apparent hinge point a little less than 1 km from the glacier terminus (Fig. 6). Does that correspond to something obvious on the ground?

What we mean to say here is that the spatial pattern of acceleration is rather uniform over the tongue – there is no 'surge front' travelling down-glacier, as has been observed in some other Karakoram Glaciers (e.g. Quincey 2011, 2015). We shall word it slightly differently, p.12, l.19–24:

"In the 2.5 years before surge onset, a gradual but clear acceleration occurred, greatest over the middle of the glacier tongue (between km 3 and km 6) with an increase in velocity from 0.1 m d^{-1} in winter 2011/12 to over 0.4 m d^{-1} in winter 2013/14 (Fig. 6). The location of the maximum velocity moved from above the confluence at km 10 at the end of 2011 to over the glacier tongue at km 5 in 2013/2014. Apart from this early shift, the spatial pattern of acceleration over the glacier tongue was quite uniform with no evidence of a surge front of acceleration moving down the glacier, as observed for some other Karakoram glaciers (Mayer et al., 2011; Quincey et al. 2015)."

The almost negligible acceleration over the lowest 1km of the glacier (resulting in this apparent 'hinge point' above which acceleration becomes evident) arises because horizontal flow is impeded by the mountain flank against which the glacier terminus pushes. This is why we observe so much thickening at the terminus, rather than horizontal advance. There is a conversion to vertical velocity which is not visible in our horizontal velocity assessment.

Fig. 12: The depression in the Dec. 2015 profile is very interesting. Do you think it could be the result of a subglacial lake drainage? Sometimes these are quite recognizable in surface crevasse patterns.

The suggestion that the surface depression could have come about through the drainage of a subglacial lake is an interesting one. However, after looking again closely at crevasse patterns over the area, we don't see any evidence of subglacial lake drainage. There are very distinctive transverse crevasses across the steep slope immediately up from where the depression formed after the surge. However, these are rather indicative of extensional stress in the flow direction, and their enlargement after the surge is likely a result of the rapid steepening over this part of the glacier as mass is removed from the reservoir area at the bottom of this steep slope (see Fig. 1 at the end of this document). We think that the depression forms because of the divergence in speed between the glacier tongue below and the tributary above, causing 'emptying' of the reservoir area during the surge. A very similar formation was observed at the Belvedere Glacier in Italy, after a surge of the glacier tongue away from the steeper upper slopes in 2000/2002 (Haeberli et al., 2002; Kääb et al., 2004, page I/70).

Could you say a bit more of the relative role of the three tributaries to the surge? The elevation change figures indicate that perhaps all tributaries are involved in the surge? Is that also borne out in velocity evolution? In Alaska, there is distinctly different behaviours of tributaries (leading to the famous looped moraines, e.g. Clarke, 1991, J.Glac.). For a reader like me it would be interesting to know whether tributaries here play a similar role or not.

Looped moraines are expected when tributaries surge into a non-surging part of the glacier, or two joining branches surge at different times. In the case of Kyagar glacier it seems to be the glacier tongue below the confluence which is surging away from the tributaries and we do not see any evidence that the tributaries themselves surge independently. The video provided in the discussion response to the review very nicely shows the lack of looped moraine formation (this video is also added as a supplement to this authors response). We will add a short explanation for the absence of looped moraines to make this clear in our discussion (see text added in response to the next comment).

p.23, l.24/25: You state that only the glacier tongue participated in the surge. This is based on the obvious velocity signature. But the elevation changes clearly show that the whole glacier is involved in the surge cycle.

The greatest acceleration was observed over the glacier tongue, but the main evidence which leads us to believe that the surge behaviour predominately occurs over the glacier tongue was the pattern of mass distribution change from the DEMs. The instability which develops during quiescence is caused in part by the buildup of mass at the top of the surging area, which in the case of Kyagar Glacier is at the bottom of the tributaries/top of the glacier tongue. It is the glacier tongue which develops the characteristic steepening during quiescence and massive redistribution during the surge. On the other hand, the tributaries don't show such irregular behaviour. They experience slight thickening all over during quiescence (and large thickening at the base of the western tributary, the main reservoir area), and slight thinning over the surge (again, large thinning only over the reservoir area). We consider the slight acceleration and thinning of the tributaries during the surge as a 'side effect' of the glacier tongue surge. Although we don't consider the tributaries as primarily surging, they are involved through providing mass to the reservoir areas and are affected by the surging tongue. We will amend the text at p.23, l.24/25 to reflect this:

"The spatial pattern of acceleration and elevation change over Kyagar Glacier provides further information about the nature of the surge, in particular that it was the tongue of the glacier which primarily underwent surging, evidenced by the velocity increase (Fig. 9) and the steepening of the profile over the glacier tongue during quiescence (Fig. 12). The build-up of an ice reservoir at the confluence represents the intersection between the surging tongue and the tributaries, which maintain more steady flow and support the recharge of the ice reservoir during quiescence. We note also that looped moraines do not form at Kyagar Glacier because there is no surging up upper tirbutaries into a non-surging part of the glacier. "

Response to review from Christoph Mayer

We would like to thank Christoph Mayer for his review. It is particularly useful to have this input given his familiarity with the surge of the nearby North Gasherbrum Glacier. We address each of his points and outline the corresponding changes to the manuscript.

There are only a few minor points I want to raise in order to hopefully improve the paper. Specific remarks:

P. 2, l. 1-3: I do not agree that the nature of glacier surging in High Mountain Asia is unknown. The mechanisms are described for different glaciers across the Karakoram and the Pamir. The recent collapse of the glaciers in Southern Tibet, just reveals that there is more to investigate about accelerating glaciers besides the known surge phenomena.

Perhaps the statement was a bit of an exaggeration as there have been a number of detailed studies

on surging in the region, so we have adjusted the text accordingly. By including the reference to the Tibet glacier collapse example we want to point out that there can still be 'surprises' related to glacier instabilities in the region.

"While surging glaciers in North America and Svalbard have been investigated in considerable detail, the large concentration of surge-type glaciers existing in the central Asian mountains, including the Karakoram (Copland et al, 2011) have been studied less extensively. Improved understanding of surge glacier dynamics in this region can assist anticipation of glacier behaviour and hazard development in the future. The recent unprecedented collapse of two surging glaciers in Tibet (GAPHAZ, 2016) highlights the potentially unexpected nature of glacier instabilities in the region."

P. 3, l. 4-11: This is a truly interesting relation between GLOF and surge timing. If you state that GLOFs are generally linked to the active surge phases, it might be worthwhile to mention Hoinkes (1969) who describes one of the very few other situations where the GLOF occurrence is clearly linked to surge activity: H.C. Hoinkes, 1969, Canadian Journal of Earth Sciences, 6(4), 853-861, doi:10.1139/e69-086

Thank you for the suggestion, this was an interesting read and we shall include a brief reference to it at p.3, l.11:

"Recurring GLOFs linked to periods of glacier surging have also been observed for other surging glaciers (e.g. Hoinkes, 1969)."

P. 3 l.32: It is preferably to use "North Gasherbrum Glacier" in order to distinguish from "South Gasherbrum Glacier" which flows into the Baltoro Glacier system.

Thank you for the clarification, we will use the name North Gasherbrum Glacier.

P.3: There should be a note in the Introduction that the glaciers of the upper Shaksgam valley seem to be prone for surging, because apart from Kyagar and North Gasherbrum Glacier also Urdok Glacier clearly shows signs of former surge activity (e.g. Kotlyakov, 1997; Copland et al., 2011).

This is a good point which we will include in the discussion (rather than the introduction) p.23, l.34:

"The fact that at least three of the five closest downstream neighbouring glaciers also experienced surging (Copland et al. 2011; Mayer et al. 2011; Quincey et al. 2015) also indicates possible locational influences on surging, for example due to local climatic characteristics (Sevestre and Benn, 2015)."

P. 5, l.9: Is the monitoring station 600 m upstream, or 500 m as noted in the caption of Fig. 3?

This will be changed to "about 500m upstream" in both instances. 500m is the best estimate of the distance of the station from the upstream ice margin of the terminus, although it is an approximate value because the position of the terminus is not constant.

P. 6, l.23: What is the reason for progressively updating the master scene for the TanDEM-X data?

A different co-registration algorithm was used for TanDEM-X data, one which updates the master scene as an average of all previously co-registered scenes, to reduce speckle and temporally average snowmelt and glacier movement. We shall mention this:

"For TanDEM-X, another co-registration algorithm was used where the master was updated progressively as the average of all previously co-registered in order to temporally smooth out moving

features or strongly changing patterns (e.g. snowmelt)."

P.7: Are you sure that the lake is only formed during surge phases?

Not at all. In fact we are quite sure that a lake can also form when the glacier is not actively surging (e.g. Fig. 2, 2009), but surging causes larger potential lake size and more probable lake formation. Periods of larger and more frequent outbursts seem to coincide with periods of suspected surging (p.3, l.7). We don't intend to give the impression that the lake exclusively forms during surge phase. Our rephrasing of the caption of Fig. 4 should avoid giving this impression:

"Images from the observation station upstream of Kyagar Glacier's terminus from (a) before and (b) during the surge. The glacier, flowing from left to right, blocks the flow of the river and causes lake formation. The dashed line in (b) indicates the ice dam height from 2012 (a), highlighting the dramatic thickening at the terminus."

P. 9, 28/29: as the SAR system is a side-looking system, the baseline is perpendicular to the flight direction. Perpendicular to the line of sight might be misleading.

The total baseline, i.e. the distance between both satellites, can be composed into three perpendicular components: along track ($B_{\parallel}$), parallel to line of sight (range offset), and perpendicular to the line of sight $B_{\perp}$). The two latter components form the across-track separation. We propose this slight reformulation:

"The phase gradient and hence the DEM accuracy depends on the perpendicular interferometric baseline $B_{\perp}$, the component of the distance between the two SAR satellites which is perpendicular to both the line-of-sight and the flight direction."

P. 10, 7-11. These two sentences are somehow describing the same thing. Maybe consolidate to one sentence.

There was some repetition which has been removed:

"The extremely rough glacier surface topography, with ice pinnacles up to 40 m high and 20-40 m apart (estimated from shadow lengths and the observations from Haemmig et al. (2014)), caused strong decorrelation and phase wraps within the coherence window of 15x15 m, meaning that DEMs could not be created over the glacier tongue with baselines $B_{\perp}$ ¡ 200 m (HoAs below 20m)."

P. 10/11, I.31-35 and Fig. 5: A comparison of a sequence of dry to wet images during the onset of snow melt gives an indication of penetration depth.

That is correct. This was done to estimate the penetration depth at the onset of snowmelt 2015 as commented in the paper p.10, l.31-33.

A sequence of wet to dry conditions will not give the same results, because it is not possible to judge the snow height by remote sensing data independently. Why should a 2 m height difference between August and December indicate a 2 m penetration depth? Given that surface melt is terminated in August (no surface height change by melt and compaction afterwards), new snow on top of this surface will result in a higher surface elevation in subsequent TanDEM-X DEMs. The height difference in this case depends on the amount of snow and the snow humidity. Given that the entire snow column above the August level is dry in December, a 2 m elevation difference only indicates that there must be at least more than 2 m of snow.

We totally agree for the case when the elevation change is positive. We forgot to mention, that we observed a negative elevation change (see answer below).

Unless there is a dynamic effect during this period. If the penetration depth is actually

2 m, the snow depth needs to be 4 m in order to produce a 2 m elevation change in the DEMs, which is rather unlikely for the end of December.

An apparent 2 m height decrease between small baseline DEMs from Aug 2015 (Fig. 5a, wet snow, low backscatter) and December 2015 (Fig. 5b, dry snow, high backscatter) indicated a penetration depth of approximately 2 m into the refrozen summer snow ONLY IF elevation decrease from subsidence and compaction and elevation increase from snowfall are neglected for the four month period between the images. We have come to the conclusion that this is an unreasonable assumption and that it's true that we can't infer much about penetration depth from the image pair with such large temporal separation. We decided to only use the image pair with short temporal separation at the onset of snowmelt. We therefore reformulate the whole paragraph from p.10 ,l.28 – p.11,l.3 as follows:

"Over the tongue of Kyagar Glacier, the backscatter intensity changed little between seasons (<5 dB), because infrequent snowfall means that the bare ice surface roughness dominates the backscatter signal from the tongue. Penetration is therefore expected to be negligible over the glacier tongue. In contrast, large seasonal changes in backscatter intensity indicate changing water content and thus varying penetration depths over the accumulation basin. Backscatter decreased by more than 10 dB at the onset of snowmelt in 2015 over the accumulation areas, and an apparent surface height increase of less than 2 m was calculated between two large baseline interferograms from before snowmelt (2015-06-02) and at the onset of snowmelt (2015-06-13). This indicates a TanDEM-X penetration depth of 2 m or less in dry snow conditions over the upper glacier. The relatively small penetration depths in the accumulation area might be a result of ice lenses formed by refreezing after strong melt events extending to over 6000 m a.s.l. in August, a phenomenon also observed by Dehecq et al. (2015). Figures showing the backscatter intensity changes are included in the supplementary material."

P. 16, Fig. 10: It might be a good idea to include the longitudinal profile again in the figure and indicate the distance along the flow line. This helps to relate the velocity profiles to the elevation changes.

We will add this to Figures 10 and 11.

P. 19, l. 15/16: Is there a reason for such large ELA changes over a short distance?

A possible reason for some of the difference in ELA between the three glacier branches could be differences in snow redistribution, wind drift, or precipitation, as temperature and radiation are likely to be very similar for all branches. However, the manual estimation of ELA from optical and radar images is rather subjective and the margins of error which we supplied in the manuscript were too low to reflect this uncertainty. After looking again at the ELA estimations is seems that an error margin of ±80m is more appropriate. We rephrase p.19, l.14-16:

"The equilibrium line altitude (ELA) estimated from the location of the snow line at the end of the ablation period observed from Landsat and TanDEM-X images, was 5350 ±80, 5400 ±80 and 5510 ±80 m a.s.l. over the western, middle and eastern branches, respectively."

P. 22, l. 20-24: How does this relate to the fact that the summer of 2013 probably has seen the most intensive melt amounts, according to the PDD calculations? After such an ablation season, I would expect the drainage system to be very effective.

2013 did have higher melt potential in summer and autumn than the three years which followed, so one would indeed expect that an efficient drainage system would be more likely to form in 2013. Perhaps the gradual increase in basal sliding which took place over the two or so years before the surge hindered the formation of an efficient enough drainage system, despite possibly larger

meltwater input in the summer before the surge started.

P. 23, l.4: A survey of existing photographs of Kyagar glacier back to the 1920s reveals that the surface of the glacier constantly is extremely rough and broken. This indicates that drainage of surface melt water into the glacier is rather effective.

Yes, the deeply pinnacled, crevassed surface is very important feature of the glacier and we also think this may assist vertical drainage. We have however noticed on the high-resolution Sentinel-2 optical images from 2016 (Fig. 2 which has also been added to the supplementary material), that some meltwater ponds form on the glacier surface between the pinnacles during summer, indicating that some meltwater at least is not well connected to vertical drainage channels (and does not percolate through the cold ice). However, we still think that there must be sufficient vertical drainage cracks/channels to allow meltwater to reach the glacier base. We will insert the following text on p.23, l.3:

"The seemingly extremely rapid response of surface velocity to the onset of surface melting indicates an efficient transfer of surface water to the glacier base which was in a critical state before the melt season started. The heavily crevassed surface, as observed during past expeditions (Mason 1928; Haemmig et al., 2014) and seen on remotely sensed images, may significantly contribute to the efficiency of vertical drainage. We note, however, that on some images supraglacial lakes are present on the glacier surface (Fig. 3 in supplementary material). This observation might indicate that surface water is not always connected with the subglacial drainage system despite of extensive crevassing. Based on the available evidence, we can however also not rule out the possibility that the supraglacial lakes are an expression of high englacial water pressures during the surge."

P. 23, l 24ff: this is also seen at other glaciers in the Karakoram. E.g. at North Gasherbrum Glacier also only the flat part below the ice fall is affected by the surge.

We add the following sentence at p.23, l.25:

"Surging confined mainly to the flatter, lower part of the glacier has been observed for a number other Karakoram surges (Mayer et al, 2011; Quincey et al., 2015)."

P. 24, l.14: as you already have calculated the PDD sums, this relates to a realistic degree day factor of about 9 mm/day.

This is a nice comparison and a confirmation of the melt estimate, thanks for bringing it to our attention. We will briefly mention it when we present the PDD results, p.19, l.22:

"The melt rate at the terminus is estimated to be around 5 m a^{-1}, according to the terminus surface elevation decrease during quiescence (Fig. 12) and the melt rate of icebergs left in the empty lake basin after lake drainage in 2009 (Haemmig et al. 2014). Combining this melt rate and an average of 552 PDDs annually gives a realistic degree-day factor of about 9 mm w.e. $^{\circ}C^{-1}$ d^{-1}."

P. 24, l. 20ff: There is an interesting discussion about discharge amount and discharge seasonality in Ng et al., 2007. Climatic control on the peak discharge of glacier outburst floods, GRL, doi: 10.1029/2007GL031426

Thanks for pointing out another relevant reference. Ng et al. (2007) show that higher temperatures during GLOF events cause higher peak discharges through increasing meltwater supply rate and lake water temperature. This effect may also impact the peak discharge during GLOFs from Kyagar Glacier, but we think the most significant factor for GLOFs from Kyagar Glacier are the glacier surge dynamics and the properties of the ice dam (height, existence of drainage channels beneath the terminus etc.). We plan to mention this reference briefly as follows at p.24, l.25:

"Meteorological factors such as air temperature during the GLOF may also influence the peak flood

discharge (Ng et al. 2007).”

References:

Kääb, A., Huggel, C., Barbero, S., Chiarle, M., Cordola, M., Epifani, F., Haeberli, W., Mortara, G., Semino, G., Semino, P., Tamburini, A. and Viazzo, G.: Glacier hazards at Belvedere Glacier and the Monte Rosa East Face, Italian Alps: Processes and mitigation, International Symposion Intrapraevent 2004 – Riva/Trient, Available: http://folk.uio.no/kaeaeb/publications/inter04.pdf, 2004

Haeberli, W., Kääb, A., Paul, F., Chiarle, M., Mortara, G., Mazza, A., Deline, P. and Richardson, S.: A surge-type movement at Ghiacciaio del Belvedere and a developing slope instability in the east face of Monte Rosa, Macugnaga, Italian Alps, Norwegian Journal of Geography, 56(2), 104-111, doi:10.1080/00291950260056422, 2002

Images:

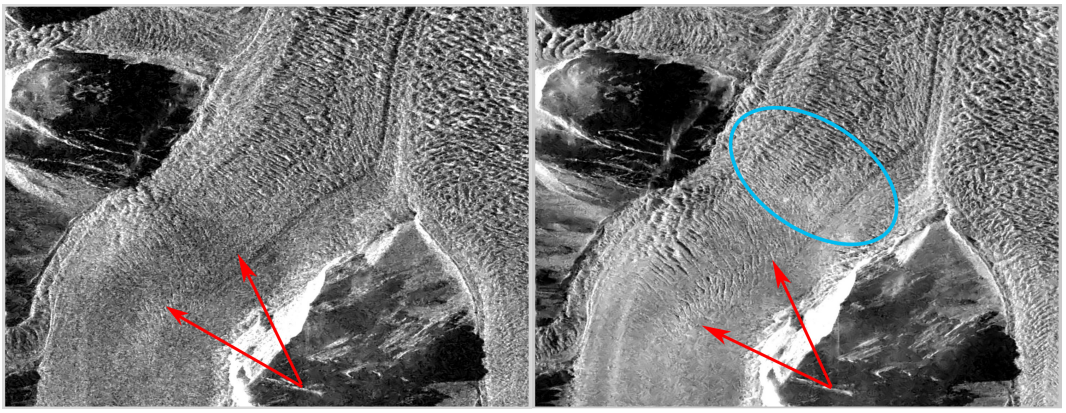

Figure 1: TanDEM-X images showing development of transverse crevasses and circling the approximate location of the surface depression which formed at around km 8.

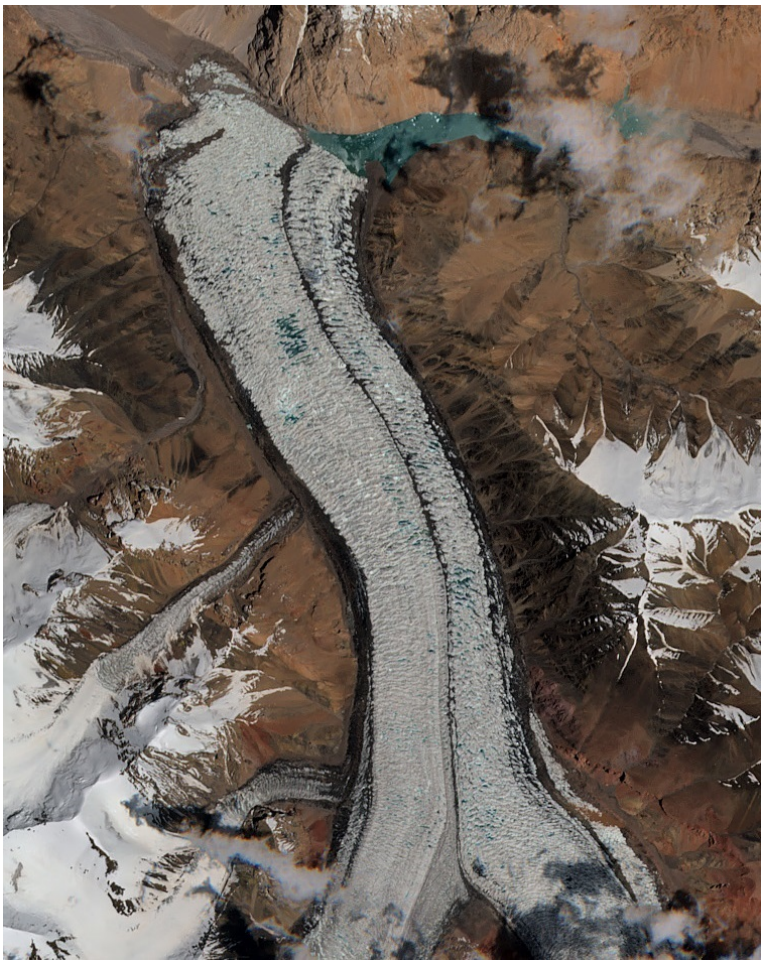

Figure 2: Sentinel-2 optical image from 27.06.2016, showing the presence of supraglacial lakes on the tongue of Kyagar glacier. This image will be included in the supplementary material accompanying the final manuscript.

Surge dynamics and lake outbursts of Kyagar Glacier, Karakoram

Vanessa Round[1,2], **Silvan Leinss**[3], **Matthias Huss**[1,4], **Christoph Haemmig**[5], **and Irena Hajnsek**[3]

[1]Laboratory of Hydraulics, Hydrology and Glaciology (VAW), ETH Zurich, 8093 Zurich, Switzerland
[2]Swiss Federal Institute for Forest, Snow and Landscape Research (WSL), 8903 Birmensdorf, Switzerland
[3]Institute of Environmental Engineering, ETH Zurich, 8093 Zurich, Switzerland
[4]Department of Geosciences, University of Fribourg, 1700 Fribourg, Switzerland
[5]GEOTEST AG, 3052 Zollikofen, Switzerland

Correspondence to: V. Round (vround@hotmail.com) / S. Leinss (leinss@ifu.baug.ethz.ch)

Abstract.

The recent surge cycle of Kyagar Glacier, in the Chinese Karakoram, caused formation of an ice-dammed lake and subsequent glacial lake outburst floods (GLOFs) exceeding 50 and 40 million m^3 in 2015 and 2016, respectively. GLOFs from Kyagar Glacier reached double this size in 2002 and earlier, but the role of glacier surging in GLOF formation was previously unrecognised. We present an integrative analysis of the glacier surge dynamics from 2011 to 2016, assessing surge mechanisms and evaluating the surge cycle impact on GLOFs. Over 80 glacier surface velocity fields were created from TanDEM-X, Sentinel-1A and Landsat satellite data. Changes in ice thickness distribution were revealed by a time series of TanDEM-X ~~DEMs~~elevation models. The analysis shows that during a quiescence phase lasting at least 14 years, ice mass built up in a reservoir area at the top of the glacier tongue and the terminus thinned by up to 100 m, but in the two years preceding the surge onset this pattern reversed. The surge ~~clearly~~ initiated with the onset of the 2014 melt season, and in the following 15 months velocity evolved in a manner consistent with a hydrologically-controlled surge mechanism~~with dramatic accelerations coinciding~~. Dramatic accelerations coincided with melt seasons, winter deceleration was accompanied by subglacial drainage, and rapid surge termination occurred following the 2015 GLOF. Rapid basal motion during ~~surging~~ the surge is seemingly controlled by high water pressure, caused by input of surface water into either an inefficient subglacial drainage system or unstable subglacial till. ~~Over 60 m of thickening at the terminus caused~~ The potential lake volume ~~to increase more than 40-fold since surge onset, to currently more than~~ increased to more than 70 million m^3 ~~, indicating that lake formation~~ by late 2016, as a result of over 60 m of thickening at the terminus. Lake formation and the evolution of the ice dam height should be carefully monitored through remote sensing to anticipate large GLOFs in the near future.

1 Introduction

Glacier surges are dynamic instabilities affecting about 1% of glaciers worldwide (Jiskoot et al., 2000). They consist of periodically alternating long quiescent phases, characterised by years to decades of slow flow, and short active surge phases, characterised by months to years of acceleration and mass transport down the glacier (Meier and Post, 1969). During the active surge phase, the glacier typically experiences dramatic lengthening or thickening at the terminus with potentially hazardous consequences, in particular ice-dammed lake formation (Harrison et al., 2014).

While surging glaciers in North America and Svalbard have been investigated in considerable detail, the large concentration of surge-type glaciers existing in the central Asian mountains, including the Karakoram (Copland et al., 2011) ~~, have been relatively little studied. The recent unprecedented collapse of two surging glaciers in Tibet (GAPHAZ, 2016) highlighted the rather unknown nature of glacier surging in High Mountain Asia.~~ are less extensively studied. Improved understanding of surge glacier dynamics in this region ~~is crucial to anticipating~~ can assist anticipation of glacier behaviour and hazard development in the future. The recent unprecedented collapse of two surging glaciers in Tibet (GAPHAZ, 2016) highlights the potentially unexpected nature of glacier instabilities in the region.

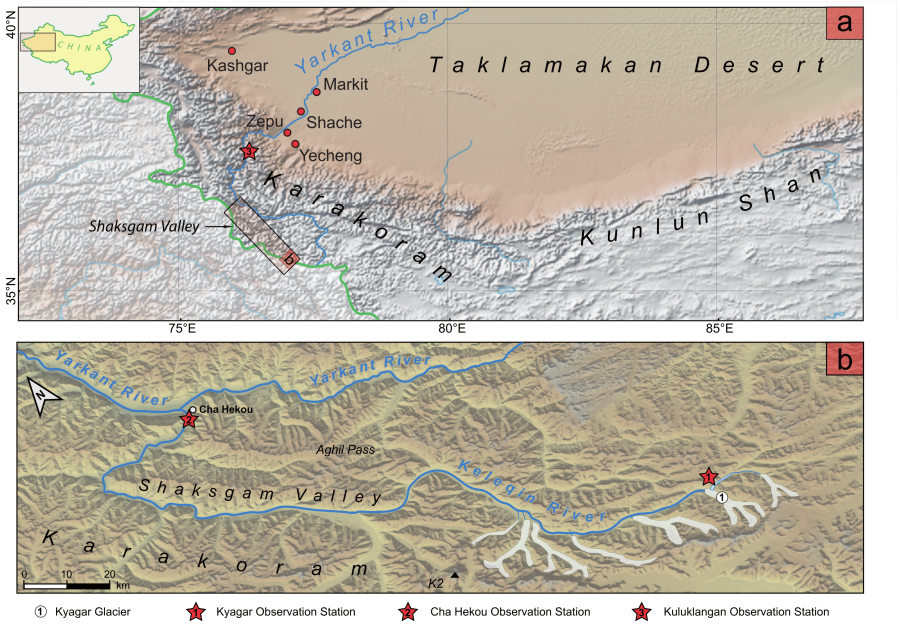

Figure 1. Location of (a) the Shaksgam Valley on the north side of the Karakoram Mountains in Western China and (b) Kyagar Glacier in the Upper Shaksgam Valley. Observation stations at Kyagar Glacier, Cha Hekou and Kuluklangon are indicated. The main flood impacts occur after the Yarkant River leaves the mountains near the Kuluklangon station.

Kyagar (Keyajir) Glacier, situated on the northern slopes of the Karakoram Mountains, occasionally causes glacial lake outburst floods (GLOFs) with devastating impacts on downstream communities along the Yarkant River in north-western China (Zhang, 1992; Hewitt and Liu, 2010; Haemmig et al., 2014). The lake forms when ice at the glacier terminus impounds the river in the Upper Shaksgam Valley. Owing to the remote location of Kyagar Glacier, about 450 km upstream of the Yarkant floodplain (Fig. 1), the origin of these floods was poorly understood in the past and they arrived without warning (Zhang, 1992; Hewitt and Liu, 2010). An automated monitoring station was placed at Kyagar Glacier in 2012 to assess lake formation (Haemmig et al., 2014), at which time there was no lake ~~because~~ as the river flowed through subglacial channels at the terminus. From mid-2014, camera images from the station showed dramatic vertical thickening of the glacier terminus ~~,~~ followed by lake formation. This rapid thickening indicated a possible glacier surge ~~. While~~ and increased the potential ice-dammed lake volume.

Although it was already recognised in the 1990s that Kyagar Glacier sometimes dammed the river in the Upper Shaksgam Valley and that there had been periods of advance or thickening in the late 1920s and 1970s (Zhang, 1992) and 1990s (Hewitt and Liu, 2010), the possibility of Kyagar being a surge-type glacier wasn't realised until recently (Gardelle et al., 2013; Haemmig et al., 2014) and no surge of the glacier has ever been documented.

~~Hazardous lake formation at Kyagar Glacier is closely linked to the glacier's surge behaviour, as increased ice thickness and deformation may push closed subglacial channels at the terminus through which the river normally flows and a higher ice dam at the terminus enlarges potential lake size. Such lakes usually fill during the summer months and empty through rapid subglacial drainage in late summer or autumn (Hewitt and Liu, 2010; Chen et al., 2010).~~ An investigation of historic GLOF occurrences from Kyagar Glacier shows that there have been three main periods of flooding in the last 60 years, with peak volumes larger than 130 million m^3 in 1961, 1978 and 1999 (Fig. 2). ~~These periods of increased GLOF activity may coincide with glacier surges and indeed there was suspected thickening between 1987 and 1999 (Hewitt and Liu, 2010) and in the late 1970s (Zhang, 1992).~~ At least the latter two of these periods coincide with periods of suspected advance or thickening. Recurring GLOFs linked to periods of glacier surging have also been observed for other surging glaciers (e.g. Hoinkes, 1969).

Surging affects both temperate and polythermal glaciers with a variety of geometries and settings (Clarke et al., 1986; Clarke, 1991; Jiskoot et al., 2000) and on vastly different timescales. The general mechanism is as follows: an unstable profile develops during quiescence, as ~~mass accumulation higher on the glacier and mass loss over~~ slow velocities fail to redistribute accumulated mass from the upper to the lower part of the glacier~~cause~~ , causing steepening of the surface and ~~increase of~~ increasing basal shear stresses, to a point at

which ~~a surge~~ surging occurs through dramatically accelerated basal sliding (Raymond, 1987). The proposed mechanisms by which the accelerated basal sliding occurs are various and not completely understood, particularly because the subglacial environment is so difficult to observe. A switch in basal thermal conditions has been identified as a surge mechanism for some polythermal glaciers, with surging occurring when cold basal conditions switch to temperate (Clarke et al., 1984; Murray et al., 2000; Fowler et al., 2001). On the other hand, for temperate glaciers and many polythermal glaciers that are already temperate at the base (Sevestre et al., 2015), surging has been explained by a hydrological switch mechanism, by which a surge occurs when the subglacial drainage system becomes inefficient, raising subglacial water pressure and facilitating rapid sliding (Kamb et al., 1985; Björnsson, 1998). Rapid deformation within subglacial till, in response to disturbance of the hydrological system within the till and increased effective water pressure, has also been proposed as an important possible surge mechanism, and is the largest uncertainty in surge understanding (Boulton and Jones, 1979; Truffer et al., 2000; Harrison and Post, 2003). In all cases, a number of positive feedback mechanisms may enhance basal motion during a surge, for instance feedbacks between deformation, frictional heating and subglacial water pressure (Weertman, 1969; Clarke et al., 1984; Sevestre et al., 2015).

Glacier surging in the Karakoram region has mainly been studied by satellite remote sensing, ~~owing~~ due to the difficulty of field access~~, in particular to identify surge glaciers through~~ . Glaciers have been classified using visible morphological features (Barrand and Murray, 2006; Copland et al., 2011) and ~~to observe surge dynamics~~ surge dynamics have been observed through surface velocities (Quincey et al., 2011, 2015; Mayer et al., 2011), producing some contradicting conclusions on surge mechanisms. Quincey et al. (2011) interpreted a lack of seasonal control on surge initiation as an indication of thermally controlled surges, whereas Mayer et al. (2011) proposed a hydrological switch mechanism for ~~Gasherbrun~~ North Gasherbrum Glacier. Quincey et al. (2015) concluded that Karakoram glacier surging must be quite heterogeneous with a spectrum of surge mechanisms at play, having observed surges exhibiting a surge-front like down-glacier acceleration as well as surges showing simultaneous glacier-wide acceleration. In the nearby West Kunlun Shan, two glacier surges showed a clear seasonal modulation of velocities during the active phase with winter velocities up to 200% higher (Yasuda and Furuya, 2015). The main limitations of these studies were data gaps meaning that various stages of the surge development, such as surge initiation, weren't observed, and changes to ice mass distribution during surging also weren't investigated. For such an investigation, digital elevation models (DEMs) from before and after the surge would be required.

In this study the combination of optical and synthetic aperture radar (SAR) satellite data reveals the lead up, the onset and termination of the surge, as well as velocity modulations in relation to the seasonal cycle during the surge phase. A DEM time series exposes the ice mass distribution changes caused by the surge and allows us to examine the mass build-up which ultimately drives the surge. Our analysis of the most up-to-date available satellite tools provides a synthesis of the dynamics of a Karakoram glacier in unprecedented detail, showing the relationships between surging and external factors such as seasonal melt cycles and lake drainage events.

In addition, we assess the impact of surging on the GLOF hazard posed by Kyagar Glacier in the recent past and into the future. GLOF hazard is largely determined by the lake volume and its drainage rate (Björnsson, 2010). The presented time series of glacier DEMs allows for the estimation of the potential lake volume and projection of potential GLOF volumes in the near future, and high-resolution satellite images reveal the drainage mechanism.

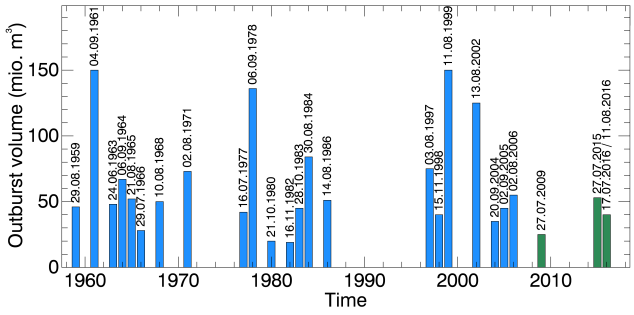

Figure 2. Historical GLOF volumes from Kyagar Glacier since the 1960s. Volumes from 1959 – 2006 are redrawn after Zhang (1992) and Chen et al. (2010). Volumes from 2006 – 2016 are estimated from lake extent on satellite images.

2 Study site and data

2.1 Study site

Kyagar Glacier is a polythermal glacier spanning from 4800 to over 7000 m a.s.l., consisting of three upper glacier tributaries 6–10 km in length which converge to form an 8 km long glacier tongue, approximately 1.5 km wide ~~(Fig. 3, Haemmig et al., 2014).~~ (Fig. 3). The total glacier area is 94 km^2 (Randolph Glacier Inventory Version 5.0, 2015) and the average surface slope is approximately 2° over the tongue and 4.5°–20° over the branches above the confluence. The surface of the glacier tongue is characterised by ice pinnacles (Fig. 4) up to 40 m high and as narrow as 10 m, indicating cold ice and low shear deformation (Haemmig et al., 2014).

The tongue of Kyagar Glacier is most likely carved into the brown/black shales and cherty limestones of the 3 km thick Perminan-Jurassic Shaksgam sedimentary formation, while the mountain range forming the southern margin of the glacier catchment consists of the Aghil formation lime-

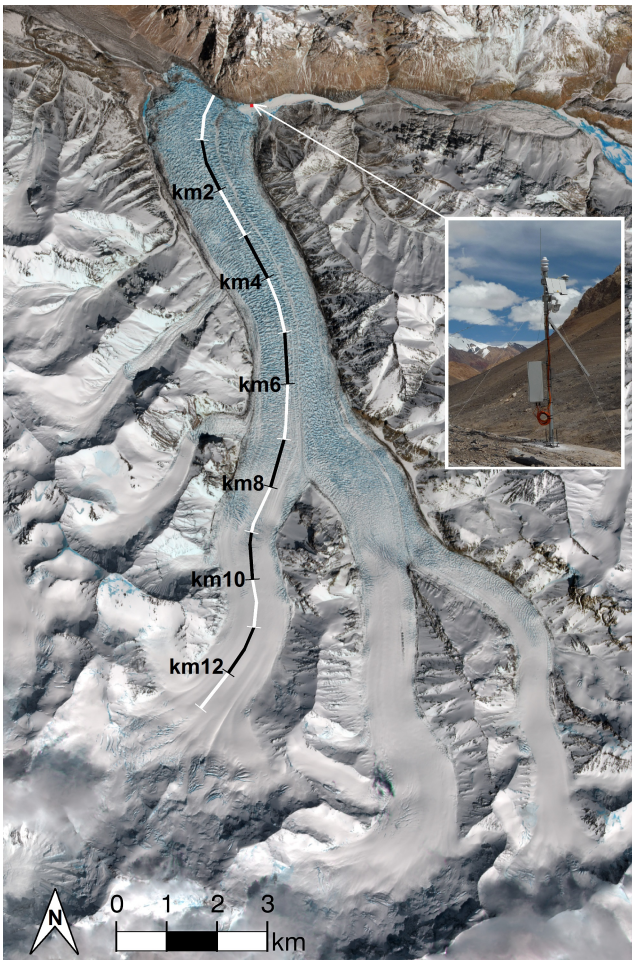

Figure 3. Optical image of Kyagar Glacier on 29.03.2016 from the ESA Sentinel-2A satellite. The glacier-dammed lake of approximately 5 million m^3 is visible to the east of the glacier terminus. The curved scale bar up the west branch indicates the longitudinal profile used for surface velocity and elevation analysis, and the inset shows the monitoring station located about 500 m upstream of the glacier terminus.

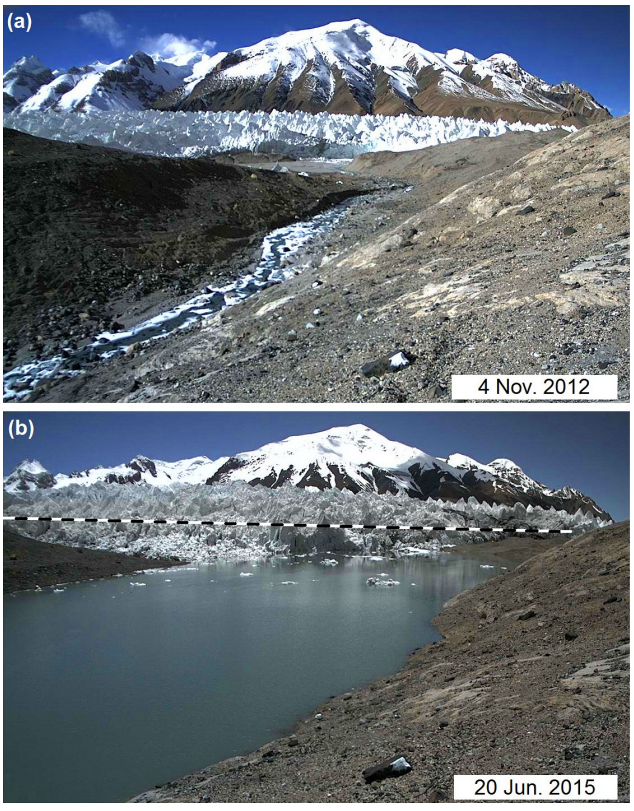

Figure 4. Images from the observation station upstream of Kyagar Glacier's terminus from (a) before and (b) during the surge. The glacier, flowing from left to right, blocks the flow of the river and causes lake formation~~during the surge~~. The dashed line in (b) indicates the ice dam height from 2012 (a), highlighting the dramatic thickening at the terminus. *Images: GEOPRAEVENT AG.*

stone and perhaps dolomite (Desio et al., 1991). The Shaksgam Valley follows the Shaksgam fault which passes under the terminus of Kyagar Glacier (Searle and Phillips, 2007).

Fieldwork at Kyagar Glacier is limited because of its remoteness and political restriction of access. Since a Sino–Swiss expedition in 2012 (Haemmig et al., 2014), in situ observations became available from an automated monitoring station ~~600~~about 500 m upstream of the Kyagar Glacier terminus (Fig. 3), which operated from 7 September 2012 until being drowned by the growing lake on 29 June 2015. ~~According to this monitoring station, air temperatures typically range between 0 and 10°C in summer and −15 and −5°C in winter.~~ The northern Karakoram is largely influenced by westerly weather patterns and snow accumulation mainly in winter, while rainfall (at lower altitudes) peaks between May and September (Kapnick et al., 2014). Balanced or slightly positive mass balances for Karakorum glaciers between 1999–2011 (Gardelle et al., 2013) contradict global trends of decreasing glacier mass balance in line with global warming, but may be explained by regional increases in winter precipitation (Kapnick et al., 2014).

2.2 Data

In situ data from the automated observation station included daily camera images of the glacier terminus, showing the upstream face of the ice dam (Fig. 4)~~as well as a wide 'fish eye' view of the lake basin~~. Meteorological variables included air temperature and precipitation amount and type, among others, recorded at hourly intervals until the station became submerged on 29 June 2015. Further meteorological data and river water level measurements were available from monitoring stations on the Yarkant River located at Cha Hekou and Kuluklangon, 190 and 500 km downstream from Kyagar Glacier, respectively (Fig. 1).

Three different satellite systems were used to determine surface velocities from the end of 2011 to mid-2016: the SAR

systems Sentinel-1A ~~(S1A)~~ and TanDEM-X and the Landsat-8 optical system. TanDEM-X is a formation of two tandem satellites, TanDEM-X and TerraSAR-X, data from both of which are used for all velocity and elevation analyses. In addition, Sentinel-2 optical images were used for visual assessment of lake formation but not for velocity analysis. Acquisition details of the three main satellite systems are presented in Table 1 (for a complete list of acquisitions see supplementary material).

3 Methods

3.1 Image co-registration

All satellite scenes were co-registered to a common master scene to allow ~~for~~ accurate comparison of images from the same orbit. The master scene for ~~S1A~~ Sentinel-1A and Landsat-8 images was the first available image from each orbit~~, while for~~ . For TanDEM-X, another co-registration algorithm was used where the master was updated progressively as ~~an~~ the average of all previously co-registered ~~slave scenes~~ scenes in order to temporally smooth out moving features or strongly changing patterns such as snowmelt. The scenes used for image co-registration covered an area of approximately $30 \times 50\,\mathrm{km}^2$ extending north from Kyagar Glacier~~. Local offsets with sub-pixel accuracy~~ , over which local offsets were calculated for patches of 512×512 ~~pixels~~pixel^2. To remove offsets resulting from patches covering moving glaciers, a planar function was fitted to the offset-fields and large outliers were removed, before again fitting a planar function to the filtered offset fields. The ~~co-registered slave~~ scenes were then resampled according to the final fitted function, resulting in a stack of images with sub-pixel co-registration accuracy.

3.2 Glacier surface velocity

Glacier surface velocities were determined using offset tracking, through which the ground offset between corresponding patches of co-registered repeat-pass satellite image pairs is computed (Strozzi et al., 2002; Luckman et al., 2007). ~~Patch-wise intensity~~ Intensity cross-correlation was applied to ~~pairs of SAR images. For~~ paired patches from the SAR images, while for Landsat optical data ~~,~~ phase cross-correlation was used to better deal with variable illumination conditions (Zitova and Flusser, 2003). The resulting offset field covering the glacier and its surroundings was then converted to surface velocity by dividing by the elapsed time between the paired images and scaling by ground range resolution. Longitudinal velocity profiles were determined along a manually determined central glacier flowline (as shown in Fig. 3) in the velocity offset patch coordinates.

The patch size and spacing are presented in Table 2. Patch sizes were selected to optimise the superior correlation ability of larger patches with the superior spatial resolution of smaller patches. Larger patches were required for the SAR systems, despite their finer resolution, to compensate for radar speckle. Velocity fields were filtered to remove offsets calculated with low correlation quality, as determined by the height of the correlation-function peak over the noise. Offsets with high divergence from ~~neighboring~~ neighbouring values and outliers with velocities 50% larger than the maximum offset over the glacier were also removed.

The accuracy of the offset tracking procedure was assessed by calculating the patch offsets over a $1 \times 2\,\mathrm{km}^2$ area of stable ground next to the glacier terminus. Since no offsets are expected over stable ground, offsets represent local inaccuracies in the co-registration of images caused by slight changes in imaging geometry and, hence, scene projection, as well as the inherent inaccuracy in the sub-pixel determination of the correlation-function peak. The root-mean-square error for the offsets over stable ground was 0.08 pixels or less for almost all the used image pairs from the three satellite systems, similar to the 0.05 pixel error estimated by Strozzi et al. (2002). ~~Larger errors were experienced for some Sentinel-1A scene pairs, in which there were slight changes in imaging geometry and in particular erroneous east-west offsets resulting from warping by the Ground Range Detected projection to a terrain height varying strip-wise in the azimuth direction (Bourbigot et al., 2016, p. 12).~~

~~The glacier surface was assumed horizontal when converting pixel offsets to ground velocities. The subsequent velocity error from this assumption~~ The velocity difference from assuming a horizontal surface for velocity calculations was only about 0.06% over the 2° sloping glacier tongue and 0.4% over the 5° slope just above the confluence. Due to the side-looking radar imaging geometry, steep slopes in the range direction ~~show distorted~~ result in a different pixel spacing hence biased velocities. However as the glacier is not very steep and flows predominately in the azimuth direction, this is not a problem.

3.3 Digital elevation models

Digital elevation models were derived using data from the TanDEM-X satellite formation (Krieger et al., 2007, 2013) using single-pass SAR interferometry. SAR interferometry allows accurate DEM generation if the absolute interferometric phase can be successfully determined from the wrapped interferometric phase measured between 0 and 2π. Determination of the absolute phase requires phase unwrapping algorithms to be applied to the interferogram (e.g. Goldstein et al., 1988; Zebker and Yanping, 1998). ~~Phase~~ The phase unwrapping can be simplified by first subtracting a synthetic interferogram, based on a reference DEM, ~~before phase unwrapping and adding the synthetic interferogram back to the unwrapped interferogram~~ and adding it back after unwrapping is completed (e.g. Dehecq et al., 2015). ~~Subtraction of the reference DEM also helps minimising~~ This

Table 1. Summary of data products acquired by the three listed satellite systems used for this study

	TanDEM-X	Sentinel-1A	Landsat-8
Authority	DLR	ESA	USGS
Data access	proposal XTI_GLAC6780	Open online	Open online
First data available	January 2008	October 2014	2013 (1972 older versions)
Spectral band (wavelength λ)	X-band (3.1 cm)	C-band (5.4 cm)	visible - IR (0.43 – 12.51 μm)
Processed data product	CoSSC (Level 1b)	GRDH IW (Level 1)	Panchromatic (B8) and NIR (B5)
Sampling resolution (m^2)	2.02×2.18 [1)] (75D[2)]) 2.17×2.21[1)] (98A[2)])	10×10 [3)]	15×15
Orbit height	514.8 km	693 km	705 km
Incidence angle θ	42.2–43.5° (75D) 38.2–39.5° (98A)	32.1-32.3°	90°
Acquisition time (UTC) [5)]	00:54 (75D) 12:46 (98A)	00:57 (descending) 00:49 (descending)	05:29[4)]
Orbit revisit	11 days	12 days	16 days

1) single look complex (SLC) single-look sampling resolution (range × azimuth).
2) 75D: orbit 75 descending (flying north to south), 98A: orbit 98 ascending (flying south to north); both having the view direction to the right.
3) Ground Range Detected (GRD) multi-looked resolution (range × azimuth).
4) Orbit: Path 148, Row 35.
5) Local daytime at Kyagar Glacier on 21. June 2016: sunrise: 23:36 UTC; sunset: 14:10 UTC.

Table 2. Patch size and patch spacing used for velocity determination.

	Patch size		Patch spacing	
	(pixels)	(meters^2)	(pixels^2)	(meters)
TanDEM-X	256×256	512×512	32	70
Sentinel-1A	64×64	640×640	18	180
Landsat	32×32	480×480	12	180

can help minimise phase-wrapping errors which can easily be recognised in the interferograms when an accurate reference DEM is used. If the phase difference to the measured data does not exceed 2π, phase unwrapping can even be avoided entirely.

The phase gradient and hence the DEM accuracy depends on the perpendicular interferometric baseline $B_\perp$, ~~which is the across-track separation between both SAR sensors (here the satellites TerraSAR-X and TanDEM-X) perpendicular to~~ the component of the distance between the two SAR satellites which is perpendicular to both the line-of-sight and the flight direction. Large baselines provide a better height accuracy with phase cycles of 2π corresponding to smaller height of ambiguity (HoA, see p. 3320 and Eq. 37 in Krieger et al., 2007), but on the other hand large baselines are more prone to phase unwrapping errors and signal decorrelation due to scattering volumes (Zebker and Villasenor, 1992) and ~~also due to~~ noise contained in the reference DEM.

The ~~DEMs~~ reference DEM used for this study ~~were generated with the help of a reference DEM, based on the~~ was composed from the 30 m resolution Shuttle Radar Topography Mission (SRTM) DEM (global version 3.0, 2015)~~which was updated and corrected by~~ , and the average of eight TanDEM-X DEMs from orbit 75D between 12 Oct. 2015–28 Dec. 2015. Phase unwrapping errors could be avoided due to the very short baselines of 19–29 meters giving large ~~HoAs~~ HAs of 250–400 m. ~~The interferograms were filtered using the adaptive interferogram filter proposed by Goldstein and Werner (1998)~~For noise reduction, an adaptive filter was applied to the interferograms (Goldstein and Werner, 1998). After phase unwrapping and conversion to height, the height corrections were averaged and added to the SRTM DEM to form the reference DEM which was downsampled to a resolution of 8×8 m^2. DEMs for each acquisition from orbit 75D were created by converting the phase difference against the reference DEM into a height change Δh, which was then added to the reference to obtain an absolute DEM for each acquisition date.

~~DEMs over the tongue of the glacier could only be calculated with baselines $B_\perp$ <200 m because the pinnacled surface structure of Kyagar Glacier caused such a strong decorrelation in the SAR interferograms that no reliable phase values could be extracted. The strong decorrelation was caused by the~~ The extremely rough glacier surface topography, with ice pinnacles up to 40 m high and 20–40 m apart (estimated from shadow lengths and the observations from ~~Haemmig et al. (2014)), which cause frequent~~ Haemmig et al., 2014), caused strong decorrelation and phase wraps within the coherence window of 15×15 m^2 for large baselines, meaning that DEMs could not be created over the glacier tongue with baselines $B_\perp$ >200 m (HoAs below 20 m~~($B_\perp$ >200 m~~).

The generated DEMs contain errors from processing uncertainties as well as from microwave penetration into snow. Processing uncertainties include phase noise due to low correlation in the interferograms, global offsets due to geometric errors, and errors of the SRTM DEM. Errors due to phase noise were estimated from the ~~standard deviation~~

differences between the eight DEMs used ~~to form~~ for the reference DEM. The standard deviation was below 4 m~~for 90% of pixels with coherence values > 0.3 (mean standard deviation 2.5 m) and global offsets were below ±1 m~~. The SRTM DEM is specified with an absolute vertical accuracy of about 10 m (Farr et al., 2007), but for comparison of DEMs systematic vertical shifts or tilts were corrected for by referencing DEMs to a common reference height ~~such that the height difference in the flat valley bottom~~ of flat terrain near the tongue of Kyagar Glacier~~was zero~~. The remaining relative error between different DEMs was estimated from four flat valley planes and resulted in a maximum height error of ± 1 m (standard deviation 0.65 m).

~~TanDEM-X radar backscatter images highlighting differences in backscatter intensity in (a) summer versus (b) winter. In the upper accumulation basin (white square at bottom of image) the dark areas in August 2015 (a) indicates low backscatter intensity from wet snow, while the high backscatter intensity in winter 2015 (b) indicates dry snow. A 2 m height difference in the area indicates approximately 2 m penetration into the dry snow. Over the glacier tongue (white square at top of image), little change in backscatter intensity indicates bare ice and, hence, very small penetration depth differences. Image data provided by DLR.~~

The error due to microwave penetration into dry snow can reach up to 6 m (Dehecq et al., 2015) for a microwave frequency of 9.65 GHz (TanDEM-X), but penetration is negligible over wet snow (more than 1% volumetric water content, Leinss et al., 2015, Fig. 5). Microwave penetration leads to potential underestimation of the actual surface height over dry snow and ice surfaces. For Kyagar Glacier, penetration depths of up to two meters have been estimated ~~as follows: firstly, the radar backscatter signal was analysed to distinguish~~ by distinguishing between dry and wet snow conditions based on backscatter intensity (Nagler and Rott, 1998; Small, 2012; Nagler et al., 2016), and ~~then~~ determining the apparent height difference between ~~images with wet and dry conditionswas identified (Fig. **??**).~~

DEMs from wet versus dry conditions. Over the tongue of Kyagar Glacier, the backscatter intensity ~~, and hence penetration, changed very~~ changed little between seasons (<5 dB)~~. This can be explained by the surface of the tongue being snow-free ice the majority of the time with fresh snowfall a rare event, and because the~~ , because infrequent snowfall means that the bare ice surface roughness dominates the backscatter signal ~~. Over the accumulation basin~~from the tongue. Penetration is therefore expected to be negligible over the glacier tongue. In contrast, large seasonal changes in backscatter intensity indicate changing water content and thus ~~penetration~~varying penetration depths over the accumulation basin. Backscatter decreased by more than 10 dB ~~between images 22 days apart~~ at the onset of snowmelt in 2015 ~~, and a height difference~~ over the accumulation areas, and an apparent surface height increase of less than 2 ~~m was calculated from~~ m was calculated between two large baseline interferograms from before snowmelt (2015-06-02) and at the onset of snowmelt ~~. A similar 2 m height difference was observed using small baseline DEMs from Aug. and Sep. 2015 (Fig. **??**a, wet snow, low backscatter)compared to December 2015 (Fig. **??**b, dry snow, high backscatter). These observations indicate~~ (2015-06-13). This indicates a TanDEM-X penetration depth of 2 m or less in dry snow conditions over the upper glacier~~and negligible penetration over the glacier tongue~~. The relatively small penetration depths ~~are likely~~ in the accumulation area might be a result of ~~thick firn layers and ice inclusionsin the accumulation area, as~~ strongly-scattering high-density firn with ice inclusions, formed by refreezing after strong melt events extending to over 6000 m a.s.l. in August (Supplementary Fig. 1), a phenomenon also observed by Dehecq et al. (2015). The backscatter intensity changes are shown in Supplementary Figures 1 and 2.

The penetration error in the SRTM DEM should be slightly larger than for the TanDEM-X DEMs, as the SRTM DEM was acquired with a C-band radar with 5.3 GHz (Farr et al., 2007) during winter (Feb. 2000). For C-band radars, expected penetration depths are 1–2 m into exposed ice (Rignot et al., 2001) and 5–10 m into dry snow (Rignot et al., 2001; Fischer et al., 2016). However, because in the accumulation area the penetration for X-band is <2 m, we estimate a penetration of <4 m in C-band (cf. Fig. 9 in Fischer et al., 2016), and over the glacier tongue 1-2 m.

In summary, systematic shifts are removed when comparing DEMs but differences in penetration must be considered in particular when comparing the SRTM to the TanDEM-X DEMs or when comparing DEMs from different seasons. Over the glacier ~~, tongue~~tongue, penetration errors are <2 meters and over the accumulation area they are estimated to be <4 meters.

3.4 Calculation of positive degree days

Positive degree days (PDD) at the glacier terminus were calculated as a proxy for potential melting~~, through summing the magnitude of positive air temperatures, ~~. Positive air temperature measurements were summed with each measurement weighted by the fraction of a day which ~~they represent (Vaughan, 2006)~~it represented (Vaughan, 2006), such that one ~~PDD would be one day at a temperature of ~~1~~hourly measurement of 6° ~~C~~would contribute 0.25 PDD. The hourly air temperature data from the station at Kyagar Glacier were used for computing PDDs in 2013 and 2014. Data from the downstream Cha Hekou observation station ~~(Fig. 1)~~ were used to estimate PDDs at the Kyagar Glacier in 2015 and 2016, to replace data from the Kyagar observation station which had been submerged. PDDs from the downstream station were scaled by using average monthly PDD offsets to the Kyagar Glacier station data from 2013 and 2014.

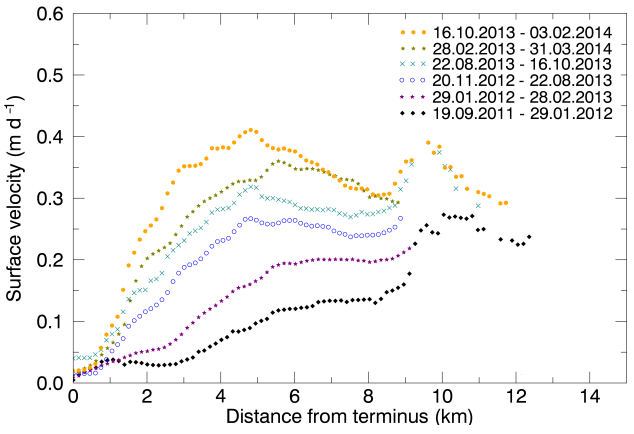

Figure 5. Longitudinal surface velocity profiles showing (from bottom to top) the pre-surge acceleration that occurred in the 2.5 years before the main surge onset. The profiles, derived from TanDEM-X data, follow the longitudinal path from Fig. 3. Gaps above km 9 indicate failed velocity calculation owing to the poor surface contrast providing no clear correlation. The labels state the time period over which each velocity calculation was averaged, in this case ranging from 2–13 months.

3.5 Lake volume estimation

Lake volumes were calculated using the DEM of the empty lake basin from TanDEM-X data acquired on 18 Aug. 2016, together with the lake extent and thus lake surface altitude from optical (Landsat or Sentinel-2) or SAR backscatter images (Sentinel-1A and TanDEM-X). In addition, the initial lake formation during the winter of 2014/15 was observed by the in situ camera, as the small initial volumes were not seen on the satellite images but were important for assessing possible subglacial drainage. Potential lake volumes ~~, and hence flood potential,~~ were estimated by calculating the lake volume which would result if the lake basin would be filled to the 90% of the ice dam height, as determined ~~by the DEMs~~ from the DEM of the glacier terminus.

4 Results

4.1 Glacier surface velocities

More than 80 surface velocity fields over Kyagar Glacier from September 2011 to August 2016 capture 2.5 years building up to the surge, the initiation of the surge in May 2014, and several periods of acceleration and deceleration in the two years following the main surge phase. Pre-surge velocity is represented in Fig. 5, while Figs. 6 and 7 are maps of surface velocity during the surge onset and main development, and Fig. 8 depicts the temporal and spatial velocity profiles over the entire study period in a 2D colour diagram. A complete set of surface velocity maps from all three satellite systems are provided in the supplementary material.

In the 2.5 years before surge onset, a gradual but clear acceleration occurred, greatest over the middle of the glacier tongue (between km 3 and km 6) with an increase in velocity from 0.1 m d^{-1} in winter 2011/12 to over 0.4 m d^{-1} in winter 2013/14 (Fig. 5). The location of the maximum velocity moved from above the confluence at km 10 at the end of 2011 to over the glacier tongue at km 5 in 2013/2014. ~~Aside from this~~ Apart from this early shift, the ~~acceleration occurred quite uniformly over the whole glacier tongue and did not show an obvious acceleration front~~ spatial pattern of acceleration over the glacier tongue was quite uniform with no evidence of a surge front moving down the glacier, as observed for some other Karakoram ~~Glaciers~~ glaciers (Mayer et al., 2011; Quincey et al., 2015). The presence of seasonal modulation could not be assessed due to the coarse temporal resolution of the six pre-surge acquisitions, but it can be seen that acceleration continued over the winter immediately before surge initiation (Fig. 5, fastest velocity profile, from Oct. 2013–Feb. 2014). This gradual pre-surge acceleration may indeed have already been under way prior to 2011, with acceleration between annual velocities from 2004/2005 to 2010/2011 based on Landsat velocity analysis by Heid and Kääb (2012).

The pre-surge acceleration appears insignificant in comparison to the main surge phase, which started at the end of April 2014. Rapid acceleration first became evident between 28 Apr. and 30 May 2014 (Fig. 6a–b), with a doubling of maximum velocity from 0.5 m d^{-1} to over 1 m d^{-1} within ~~a 32-day period~~32 days. Velocities continued increasing steadily (Fig. 6c) to a peak of almost 2.5 m d^{-1} (Fig. 6d) between the 19 Sep. and 5 Oct. 2014. The maximum instantaneous velocity is likely to have been higher than the calculated values which are averages over 16-day periods. The surge caused a six-fold acceleration in the five months following May 2014, and more than a 20-fold acceleration since 2011/12.

After the surge peak in Sep. 2014, there was a slight deceleration which continued during winter (Fig. 6e) until maximum velocities had dropped to about 1.2 m d^{-1} in April 2015. This was followed by a new phase of acceleration through May–July 2015 to almost 2 m d^{-1} in late July, slightly slower than the peak velocity in summer 2014. This acceleration came to an abrupt halt between 27 July and 7 Aug. 2015, causing the most rapid change observed with a halving of velocities over the tongue within 22 days (Fig. 7a–c). This abrupt slow-down was aligned with the lake drainage on 27 July, as indicated by the arrow in Fig. 8.

Deceleration continued over autumn 2015 and winter of 2015/16, and velocities almost returned to pre-surge levels with a maximum ~~of~~ less than 0.5 m d^{-1} in March 2016. There was a slight acceleration after April 2016 but velocities were still significantly below the previous two summers, remaining below 1 m d^{-1}.

Fig. 8, consisting of a stacked time series of velocity profiles along the glacier, shows that the surge mainly affected

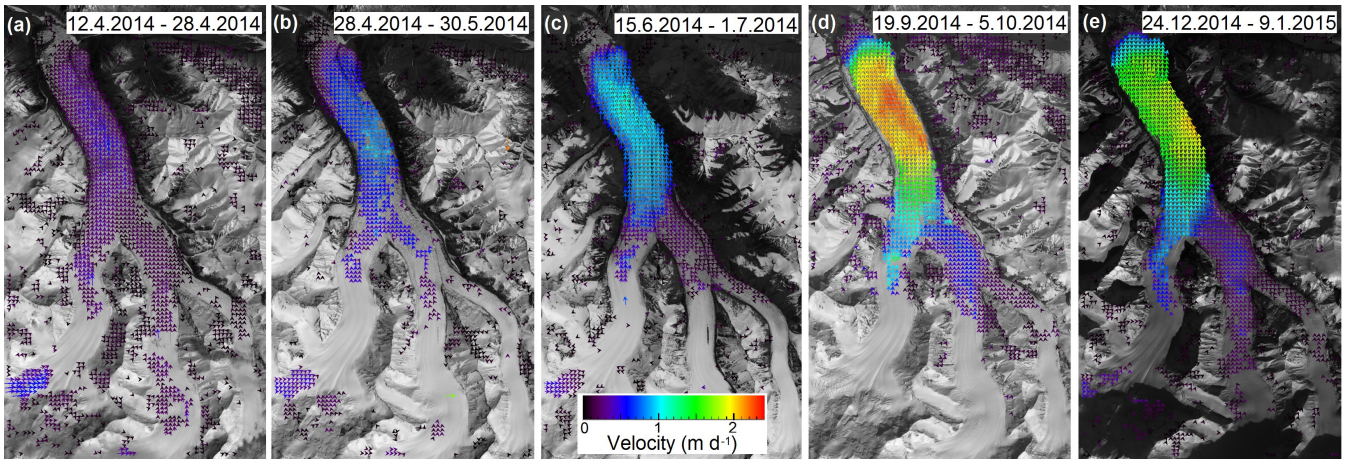

Figure 6. Velocity fields showing the onset and peak of the surge. Panels (a)–(c) show the initial acceleration between April and July 2014, (d) shows the maximum of the surge in Sep./Oct. followed by deceleration to lower velocities in winter 2014/15 (e). Background image from USGS Landsat 8 satellite data.

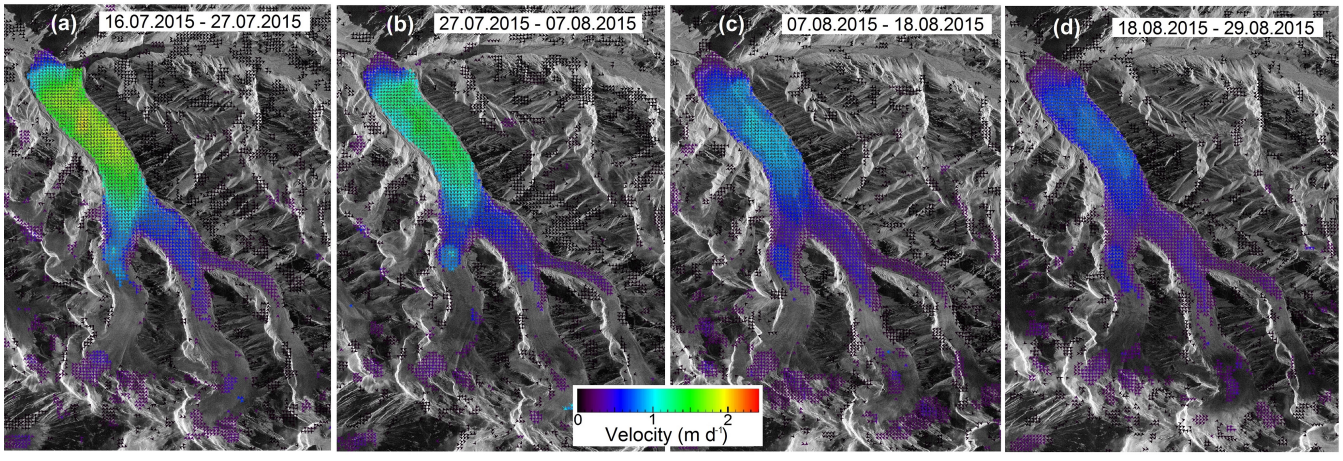

Figure 7. Velocity fields showing (a) the maximum velocity reached in 2015, followed by (b)–(d) the sudden deceleration from the end of July into August. These velocity fields were calculated from consecutive 11-day periods. Background image from TanDEM-X data provided by DLR.

the tongue of the glacier, between km 1 and km 8, while above the confluence (> km 8) the effect of the surge was small.

4.2 Glacier surface elevation

Four DEMs based on TanDEM-X data acquired before the surge (2012–2014) and eight DEMs from after the main part of the surge (Oct.–Dec. 2015) were compared with each other and with the SRTM DEM from 2000, to reveal the dramatic changes in glacier surface elevation and, hence, ice mass distribution over Kyagar Glacier caused by the surge. Maps of elevation change over the glacier during the quiescence and surge periods are shown in Fig. 9 and 10, respectively. Longitudinal profiles of surface elevation are shown in Fig. 11a and the elevation change rates in Fig. 11b.

Before the surge, between Feb. 2000 and Nov. 2012, the surface elevation decreased gradually over most of the glacier tongue at a rate of 5 m a^{-1} (Fig. 9 and Fig. 11b), resulting in an elevation loss of over 60 meters at the glacier terminus. At the same time, elevation increased over the western branch by up to 30 meters just above the confluence, while over the eastern branches the surface elevation increased more moderately with a maximum gain of 10 meters (Fig. 9). This observed pattern is typical of a surging glacier in the quiescence phase, with downwasting over the glacier tongue and ice build up in a reservoir area, which for Kyagar Glacier forms just above the confluence on the western branch.

Between 2012 and 2014, in the two years preceding the surge, there was already a slight reversal of the quiescence pattern seen in the previous 12 years, with minor elevation

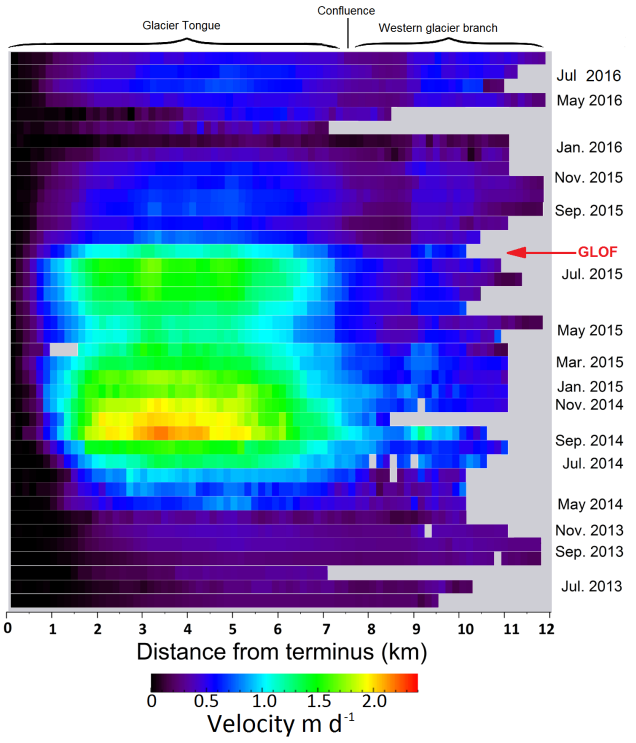

Figure 8. Evolution of surface velocity along the longitudinal profile (see Fig. 3) showing the spatial extent of the surge and how it evolved in time. The surge predominately affected the glacier below the confluence at km 8. The red arrow indicates the GLOF on 27 July 2015 and the corresponding abrupt deceleration.

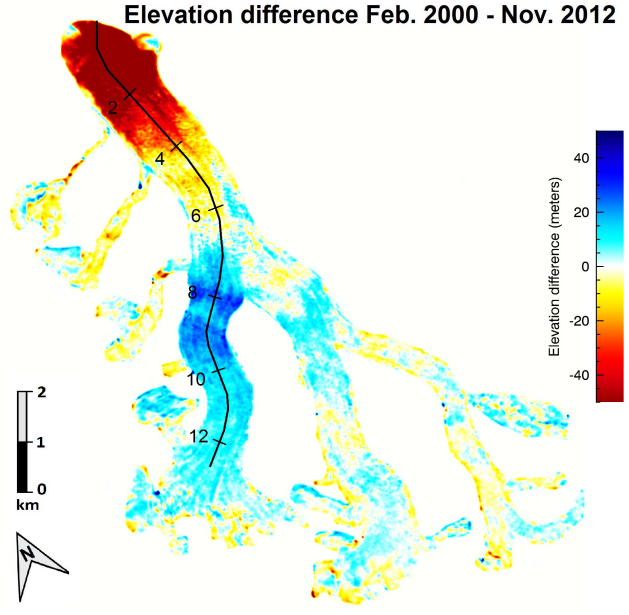

Figure 9. Glacier surface elevation changes ~~from DEM subtraction~~ between Feb. 2000 (SRTM) and Nov. 2012 (TanDEM-X). The elevation change represents 12 years of quiescence preceding the surge. The image is shown in radar coordinates for TanDEM-X data of orbit 75D, accounting for the slightly different orientation to the optical image in Fig. 3.

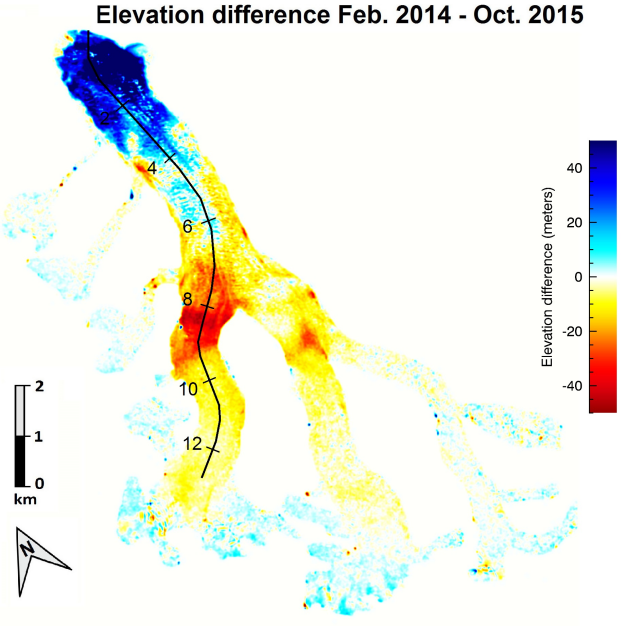

Figure 10. Glacier surface elevation changes during the surge from subtraction of two TanDEM-X DEMs from Feb. 2014 and Oct. 2015. This surface elevation change reverses the change pattern shown in Fig. 9 through only 1.5 years of surging.

loss just above the confluence and mass gain over the tongue (Fig. 11), indicating mass transport down the glacier from the reservoir. During the surge in 2014/15, this mass transport from the reservoir area intensified dramatically with ice surface elevation increasing at a rate of almost 40 m a^{-1} over the lowest parts of the glacier tongue, causing thickening in excess of ~~80~~ 60 meters at the terminus since Feb. 2014. At the same time, surface elevation decreased by more than 40 meters just above the confluence where the reservoir area formed during the quiescence. ~~These changes are typical of a glacier surge and reflect the rapid transport of ice mass from the reservoir area down the glacier, in this case causing thickening at the terminus and lower glacier tongue.~~ The mass transport~~during the surge~~, typical during a surge phase, essentially reversed the changes which occurred during the quiescence (2000–2012), such that the glacier surface profile at the end of 2015 had almost returned to that of 2000 (brown vs. blue lines in Fig.11a).

There were significant adjustments to surface slope throughout the course of the surge, particularly over the glacier tongue. In 2000, the average slope over the first eight ~~kilometers~~ kilometres of the glacier was about 1.4° and by 2012/2014 it had increased to about 2.3°. By the end of 2015, after the surge, slope had decreased again to about 1.6°.

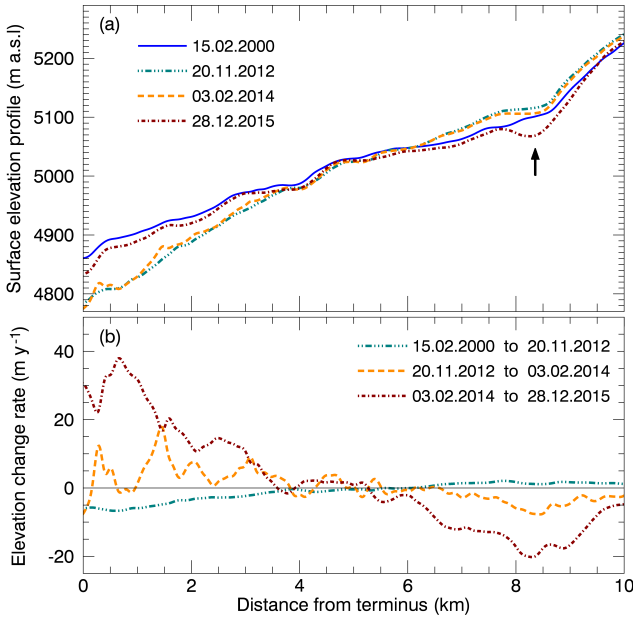

Figure 11. (a) Elevation profiles from 2000, 2012, 2014 and 2015, and (b) the rate of elevation change between the periods 2000–2012, 2012–2014 and 2014–2015. Profiles are taken along the transect indicated in Fig. ~~3~~ 9 and 10, and the black arrow indicates the location of the surface hollow remaining after the surge.

The post-surge glacier surface in Oct. 2015 showed the presence of a surface hollow, approximately 12 m deep and up to 1 km wide, at the very beginning of the western branch above the confluence just before the slope significantly steepens (Fig. 11a, indicated by arrow). Such a depression is an unusual feature but could have formed as a consequence of the surge transporting ice from the reservoir area faster than the rate of replacement from above, owing to the observed flow disparity between the tongue and the glacier branches.

4.2.1 Mass balance and equilibrium line altitude

Although not directly related to the surge characterisation, we provide a geodetic mass balance estimate for Kyagar Glacier between 2000 and 2015. The average volume difference between the SRTM DEM and eight TanDEM-X DEMs from between Oct.–Dec. 2015 was calculated and converted to mass change assuming an ice density of $850 \pm 60\,\mathrm{kg\,m^{-3}}$ (Huss, 2013). The mass balance was found to be -0.24 ± 0.22 m w.e $\mathrm{a^{-1}}$. For the uncertainty, the radar penetration difference between the SRTM and the TanDEM-X DEMs dominates and was estimated to be a conservative 3 m systematic error over the whole glacier. As the penetration for the SRTM C-band microwaves is deeper than the TanDEM-X X-band, our calculation may slightly underestimate mass loss. On the other hand, the area used for calculation (61 $\mathrm{km^2}$) missed some of the steepest portions of the accumulation area due to lack of interferometric coherence affecting DEM creation, possibly leading to an underrepresentation of the accumulation area and exaggerated mass loss. For comparison, Gardelle et al. (2013) reported an average mass balance of $+0.11 \pm 0.14$ m w.e $\mathrm{a^{-1}}$ for glaciers in the east Karakoram region between 2000 and 2008.

The equilibrium line altitude (ELA) estimated from the location of the snow line at the end of the ablation period observed from Landsat and TanDEM-X images, was 5350±~~15~~80, 5400±~~25~~ 80 and 5510±~~30~~80 m a.s.l. over the western, middle and eastern branches, respectively.

4.3 Meteorological observations

~~Data from the Kyagar meteorological station~~ Temperatures remained below 0° C between mid-October and late April according to data from the meteorological station at the glacier terminus (at 4800 m a.s.l.)~~between Sep. 2012 and Jun. 2015 revealed that temperatures remained below 0° between October and late March to late April. Melting potential predominately occurred in June, July and August with monthly positive degree days exceeding 150 PDDs in July and August 2013 and during the~~ . The warmest months, July and August, ~~average maximum temperatures were~~ experienced average daily maximum temperatures of 4–7° C ~~. Annual PDDs~~ and monthly PDDs exceeding 150 at the glacier terminus. By taking into account the glacier surface elevation and an lapse rate of about -0.006° C $\mathrm{m^{-1}}$, it can be inferred that over the whole glacier tongue, PDDs are positive between May and October, whilst over the bulk of the accumulation area (about 900 m above the terminus) melt potential was only significant from June to August. Evidence of high-altitude melt is also seen in the TanDEM-X backscatter images from August 2015 (Supplementary Fig. 1). Annual PDDs at the glacier terminus were 647° C, 481° C, 552° C and 528° C in 2013, 2014, 2015 and 2016, respectively. The melt rate at the terminus is estimated to be around 5 m $\mathrm{a^{-1}}$, according to the terminus surface elevation decrease during quiescence (Fig. 11) and the melt rate of icebergs left in the empty lake basin after lake drainage in 2009 (Haemmig et al., 2014). Combining this melt rate and the annual average of 552 PDDs gives a realistic degree day factor of about 9 mm w.e. $\mathrm{^{\circ}C^{-1}\,d^{-1}}$.

4.4 Lake formation and drainage

Images from the monitoring station at Kyagar Glacier showed that a lake initially began forming in the river basin upstream of the glacier terminus in early December 2014. During January and February 2015 the lake appeared to fill faster, before remaining at a constant size (still less than 1 million $\mathrm{m^3}$) during March. In April 2015 the lake size increased again in line with the onset of spring melting, continuing more rapidly during the summer until reaching an estimated volume of 53 million $\mathrm{m^3}$ before draining through

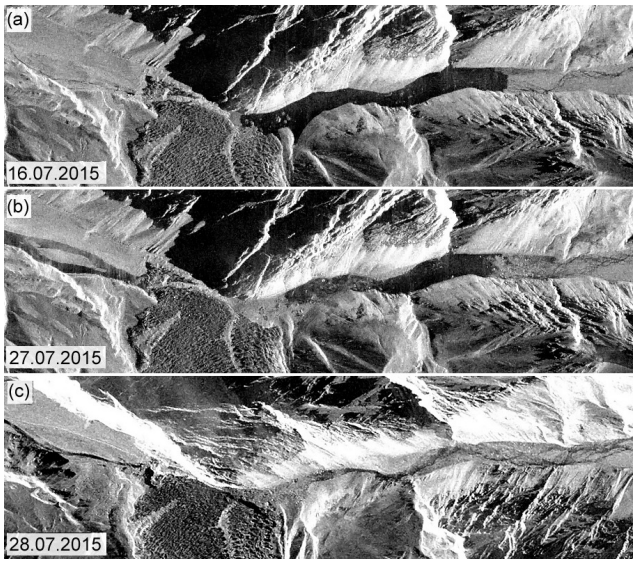

Figure 12. Radar backscatter images of the glacier terminus showing (a) the lake 11 days before drainage, (b) just after the start of drainage and (c) after the lake drainage. Lake drainage clearly occurred through subglacial channels, rather than through dam collapse or over topping. Images from TanDEM-X data provided by DLR.

subglacial channels on the 27 July 2015, as observed by TanDEM-X acquisitions (Fig. 12).

Following the drainage in July, a new lake started forming in September 2015 and remained at a volume of approximately 1.5 million m^3 between Oct. and Dec. 2015. As during the previous winter, the lake size increased between January and February 2016, from approximately 1.5 to 5.0 million m^3, and again this winter lake filling seemed to stop during March and recommence with the onset of the melting season. The lake rapidly filled during summer 2016 and reached an estimated volume of 40 million m^3 by 13 July before a rapid drainage event occurred on 17 July 2016. Almost immediately after this event, the lake ~~appeared to fill~~ filled again and reached an estimated volume of 37 million m^3 on 4 Aug before a second drainage event on 11 Aug. Lake volumes, as calculated from satellite images and the lake basin DEM, are provided in the supplementary material.

5 Discussion

Based on the results, we discuss possible surge mechanisms ~~producing~~ for the observed behaviour of the glacier before and during the main surge phase, and rule out mechanisms which contradict the observed behaviour. The effect of the surge cycle on the GLOF hazard posed by Kyagar Glacier in the past and future is assessed to provide an outlook for its hazard potential.

5.1 Surge mechanisms for Kyagar Glacier

5.1.1 Pre-surge build up

The observed pre-surge acceleration could have arisen through increased internal ice deformation and/or increased basal sliding, both of which may be expected following the steepening of the glacier tongue between 2000 and 2012 (Fig. 11a). The contribution of internal ice deformation u_d to surface flow can be estimated with the parallel-sided slab assumption with the plain strain approximation (Greve and Blatter, 2009), as

$$u_d = \frac{2A}{n+1} (\rho g \sin\alpha)^n H^{n+1}, \quad (1)$$

where the strain rate factor $A = 2.4 \times 10^{-24}$ s^{-1} Pa^{-3} (for temperate ice, a conservative estimate), ice density $\rho = 900\,kg\,m^{-3}$, Glen's exponent $n = 3$, and gravitational acceleration $g = 9.8\,m\,s^{-2}$, leaving the key variables surface slope, α, and ice thickness H (Cuffey and Paterson, 2010). Assuming a constant glacier thickness of 250 m, an estimation on the high side according to the glacier bed profile presented by Haemmig et al. (2014), the 1.4° surface slope over the glacier tongue in 2000 would result in a surface velocity of 4 mm d^{-1}. The increased slope of 2.3° in 2012 would give deformation velocities of around 18 mm d^{-1}, approximately one order of magnitude lower than the observed 0.1 m d^{-1} between 2011–2012 (Fig. 5). ~~It~~ Hence, it seems that basal motion significantly contributed to flow of the glacier tongue already prior to the surge, indicating that the base of the glacier tongue was already temperate ~~,~~ and contradicting the thermal mechanism in which a switch from cold to temperate base causes surge onset. Conditions are different above the confluence where the surface slope of around 4.5° in 2012 could cause surface velocities on the order of 0.1 m d^{-1} through internal deformation alone, in the same order of magnitude as observed velocities. Pre-surge velocities above the confluence could therefore feasibly occur in a cold-based situation through internal deformation without the contribution of basal motion. However, basal motion upstream of the confluence is not ruled out with this simple calculation.

The effect of ~~a change in surface topography~~ increased surface slope on basal shear stress, τ_b, during the quiescence can be estimated from

$$\tau_b = \rho g H \sin\alpha, \quad (2)$$

if the glacier base is assumed to mirror the surface slope (Cuffey and Paterson, 2010). If all variables except the slope are considered constant, the increase from 1.4° to 2.3° between 2000 and 2012 over the glacier tongue would have caused a 64% basal shear stress increase, from about 54 to 88 kPa. The thickness increase over the reservoir area would further increase τ_b at the upper part of the glacier tongue. Given the potential sensitivity of the subglacial hydrological

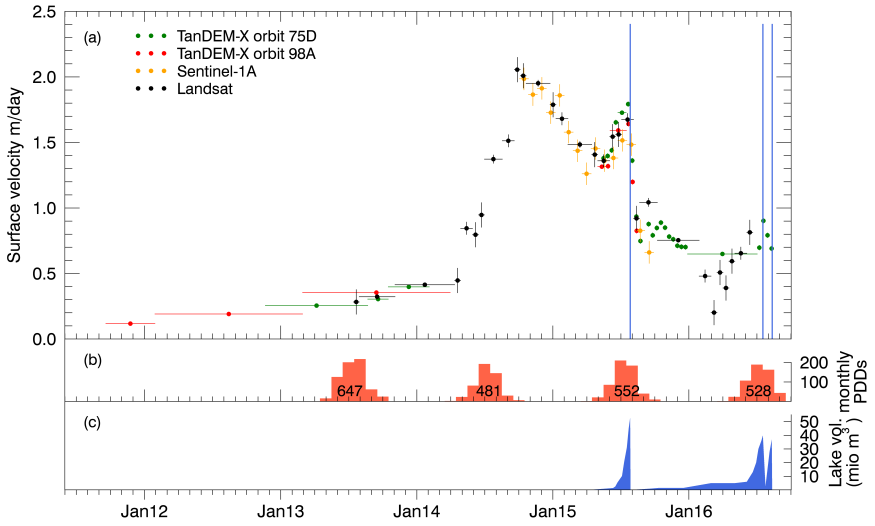

Figure 13. (a) Evolution of surface velocity at the middle of the glacier tongue (4 km from the terminus, Fig. 3) from the end of 2011 until mid-2016, with horizontal bars representing the period over which velocity was calculated and vertical bars showing the velocity uncertainty. The blue vertical lines indicate GLOF events. (b) Monthly PDDs indicated by the bars and yearly PDDs indicated by the numbers. (c) Temporal change in lake volume as calculated from lake extent on satellite images.

drainage system efficiency to basal stress (Eisen et al., 2005), the conditions at the end of the quiescence could favour a switch to an inefficient drainage system.

However, the slope began decreasing between 2012 and 2014 (Fig. 11) while velocity continued to increase. This contradicts the idea that increasing slope alone could have driven the acceleration. Positive feedback mechanisms triggered by ~~the basal stress increase~~ increasing basal stress must therefore play a role in the continued acceleration during the late quiescence, and ultimately in bringing the glacier into a critical state before surge initiation. These could include increased frictional heating enhancing melt water production and water pressure at the glacier base (Dunse et al., 2015; Weertman, 1969), or increased basal deformation closing subglacial drainage channels, thus trapping water and increasing water pressure (Clarke et al., 1984; Kamb et al., 1985). Processes within the subglacial till such as a positive feedback between till deformation, consolidation and water pressure (Boulton and Zatsepin, 2006) could also play a role.

The continuation of acceleration during winter 2013/2014 (Fig. 13), rather than another slow-down as observed by Haemmig et al. (2014) during the previous winter, may indicate the presence of an inefficient subglacial drainage system. Such winter acceleration was observed prior to the 1982/83 surge of Variegated Glacier and was attributed to the establishment of an inefficient linked cavity drainage system with higher water pressure, in part due to low water flux allowing drainage channels to close (Kamb et al., 1985).

5.1.2 Main surge phase, 2014 to 2016

The ~~presence of~~ rapid spring acceleration observed in May 2014 can be explained by the input of surface meltwater increasing water pressure in an inefficient subglacial drainage system~~during the last winterof the quiescence, as indicated by increased winter velocities, would account for the summer acceleration as the input of surface meltwater increased water pressure and facilitated the onset of the surge as observed in May 2014. Acceleration~~ , which was suspected to be present during the preceding winter. Continued acceleration through the summer could reflect increasing subglacial water pressure as meltwater input continued. The deceleration after reaching maximum velocities in Oct. 2014 indicates decreasing subglacial water pressure, perhaps through the gradual evolution of a subglacial drainage system towards the end of summer followed by declining melt water input and possible subglacial drainage. Evidence for the drainage of en- or sub-glacially stored water during wintertime comes from the observed lake formation starting in December 2014, at a time when temperatures consistently well below zero exclude surface water sources. The lake growth and, hence, the drainage of subglacial water, appeared to end in January 2015. This indicates that most subglacial water was already drained or that subglacial drainage channels closed towards the end of the winter. Closing of the subglacial channels would again put the subglacial system into a state very sensitive to surface water input and allow summer-onset acceleration again in 2015. The seemingly extremely rapid response of surface velocity to the onset of surface melting indicates an efficient transfer of surface water to the glacier base ~~and that the~~

~~glacier~~ which was in a critical state before the melt season started. The heavily crevassed surface, as observed during past expeditions (Mason, 1928; Haemmig et al., 2014) and seen on satellite images, may significantly contribute to the efficiency of vertical drainage. We note, however, that on some images supraglacial lakes are present on the glacier surface (Supplementary Fig. 3). This observation might indicate that surface water is not always connected with the subglacial drainage system despite extensive crevassing. Based on the available evidence, we can however also not rule out the possibility that the supraglacial lakes are an expression of high englacial water pressures during the surge.

The abrupt deceleration at the end of July 2015, occurring simultaneously with the lake outburst, is a more extreme example of deceleration occurring in association with subglacial drainage. It seems that the opening of subglacial channels beneath the terminus during the lake outburst triggered the reduction of subglacial water pressure and, hence, velocity beneath the whole glacier tongue within 11 days (Fig. 7). This may have occurred through the sudden formation of an efficient drainage system due to the change in boundary conditions at the terminus of the glacier, particularly the sudden decrease in water pressure as the lake level dropped.

5.1.3 Summary of surge mechanism

The various phases of the surge were facilitated by a basal motion mechanism very sensitive to subglacial water pressure, controlled by meltwater input in summer, reduced input and perhaps drainage of most of the subglacial water in early winter, and rapid subglacial drainage during the GLOF in summer 2015. It seems that the surge is well explained by the presence of an inefficient basal drainage system facilitating high subglacial water pressure, corresponding to the mechanism proposed by Kamb et al. (1985). However, ~~similar observations could also be explained by replacing~~ the seasonality observed at Kyagar Glacier is different to the often cited winter initiation associated with closure of subglacial channels in the hydrological switch mechanism (Eisen et al., 2005; Kamb et al., 1985). In the case of Kyagar Glacier, development of an inefficient drainage system in winter does not necessarily facilitate increased subglacial water pressure until the beginning of the melt season, due a lack of liquid water in winter. Surge initiation in winter should not be considered a precondition of hydrologically controlled surges (see eg. Jiskoot and Low (2011)).

We note that the idea of surge initiation through formation of an inefficient drainage system ~~with~~ as discussed in Section 5.1.2, could be replaced by that of a layer of subglacial till in which increased water pressure reduces till strength to a deformation threshold (Boulton and Jones, 1979; Cuffey and Paterson, 2010). It is likely that the tongue of Kyagar Glacier is underlain by a permeable till, owing to fine-grained sedimentary rock on which the glacier tongue lies (Desio et al., 1991; Searle and Phillips, 2007). We can not speculate further on the exact nature of the subglacial drainage system as there is no field evidence, but conclude that Kyagar Glacier is a system very sensitive to water in- and outputs during the surge, rather than being purely internally regulated.

The spatial pattern of ~~surging provides some~~ acceleration and elevation change over Kyagar Glacier provides further information about the nature of ~~Kyagar Glacier~~the surge, in particular ~~the observation that only~~ that it was the tongue of the glacier ~~participated in the surge~~ which primarily underwent surging, evidenced by the velocity increase (Fig. 8) ~~. The build up~~ and the steepening of the profile over the glacier tongue during quiescence (Fig. 11). The build-up of an ice reservoir at the confluence represents the intersection between the surging tongue and the ~~non-surging upper branches.~~ tributaries, which maintain more steady flow and support the recharge of the ice reservoir during quiescence. We note also that looped moraines do not form at Kyagar Glacier because there is no surging of upper tributaries into a non-surging part of the glacier (see supplementary video). Surging confined mainly to the flatter, lower part of the glacier has been observed for a number other Karakoram surges (Mayer et al., 2011; Quincey et al., 2015).

The distinction between these two parts of the glacier is also reflected in the glacier surface slope with the tongue being much more gently-sloped (2° vs. 4.5°). The surge behaviour ~~may stem~~ of Kyagar Glacier likely stems from the characteristics of the lower glacier, in particular its apparent inability to transport mass from the reservoir area down the glacier tongue to the terminus in a regular manner. Basal motion is necessary to transport mass from the reservoir area down the glacier tongue, but some characteristic of the ~~basal environment must cause~~ glacier causes this to occur cyclically through periods of surging. ~~Clarke et al. (1984) noted that downstream resistance to flow may be a common factor for creating glacier surges, allowing mass build-up in a reservoir area and~~ Clarke et al. (1986) noted that surging glaciers tended to have greater slope over the accumulation area and lower slope over the ablation area, and Björnsson et al. (2003) summarised that surge-type glaciers in Iceland tended to exhibit small slopes with velocities too slow to remain in balance with the accumulation rate. These factors could also apply to Kyagar Glacier. The fact that at least three of the five closest downstream neighbouring glaciers have also experienced surging (Copland et al., 2011; Mayer et al., 2011; Quincey et al., 2015) also indicates possible locational influences on surging, for example due to local topographic and climatic conditions (Sevestre and Benn, 2015).

We estimate a surge return period of around 15–20 years for Kyagar Glacier, based on the information that the last major period of advance was in the late 1990s (Hewitt and Liu, 2010) and ~~backed up by~~ the similarity between the glacier profile in 2000 and that from after the surge in 2015 (Fig. 11). The historic frequency of lake outburst flooding indi-

cates periods of increased lake formation, and therefore probably surge activity, every 15–20 years (Fig. 2). The surge return periods of other individual Karakoram glaciers have also been similarly estimated at around 15 to 20 years (Mayer et al., 2011; Quincey and Luckman, 2014), although longer return periods are also possible Copland et al. (2011).

5.2 Future outlook for Kyagar Glacier and lake formation

The potential volume of the glacier-dammed lake at Kyagar Glacier depends both on the height of the ice dam at the glacier terminus and whether the subglacial channels through which the lake drains are open or closed. Thickening of over 60 m at the glacier terminus caused potential GLOF volume to increase more than 40-fold since early 2014, to over 70 million m^3 according to the August 2016 DEM of the glacier. GLOF hazard potential is expected to remain high for a number of years as the still slightly elevated tongue velocity continues to transport mass to the terminus area, potentially increasing the height of the ice dam until mass transport to the terminus area falls below the ablation rate. The height of the ice dam is expected to decrease at an estimated rate of 5 m a^{-1} once mass transport to the terminus ceases, according to the ablation rate of the latest quiescence phase and the estimated melting rate of icebergs left in the empty lake basin after lake drainage in 2009/2010 (Haemmig et al., 2014). Unless the mass balance significantly changes, it would be expected that the next quiescence phase would last until around 2030 based on an estimated 15–20 year return period.

The size of future GLOFs depends ~~not~~ largely only on the potential lake volume, ~~but also greatly on the timing of lake drainage, as drainage may begin~~ the volume reached if the lake filled to 90% of the ice height. However the actual volume reached may be less it the lake drains before the potential volume is reached. ~~It seems that the maximum potential~~ Despite the ice dam being about 5 meters higher in 2016 than 2015, the lake volume was ~~not reached~~ less in 2016 ~~due to the outburst occurring~~ as the outburst occurred at about 85% of the ice dam height~~, meaning that smaller volumes were encountered than in 2015 despite the potential volume being larger. This may~~ . This can be explained by subglacial channels from the 2015 lake outburst providing a weaker, preferential pathway for lake drainage and thus earlier outburst in 2016 followed by a smaller second outburst. We note that GLOFs > 80 million m^3 have never been followed by a significant drainage event in the next year (Fig. 2), which perhaps indicates that large floods cause formation of subglacial channels large enough to remain open until the following year. Meteorological factors, such as temperature during the GLOF, may also influence the peak flood discharge (Ng et al., 2007).

It is important that the ~~lake size and volume~~ height of the ice dam and the lake evolution is monitored through satellite imagery each summer in the ~~next few years to~~ years following the surge, to assess imminent GLOF threat and allow affected communities to be ~~warned of the imminent GLOF threat~~better prepared for flood impacts.

6 Conclusion

Our integrative picture of the recent surge of Kyagar Glacier, built from satellite surface velocity maps, terrestrial ~~observation~~ station images and DEMs, provides an extraordinary insight into glacial surging in connection with surface hydrology and glacier-dammed lake formation and outburst. After gradual surface velocity increase through the last few years of the quiescence, the glacier entered a state highly sensitive to surface water input. Two dramatic acceleration phases occurred in concurrence with the onset of the surface meltwater production in the seasons of 2014 and 2015, indicating a surge mechanism related to the evolution of the basal hydrological system and associated changes in subglacial water pressure, rather than to an internally controlled switch to ~~warmer~~ temperate basal temperatures. Between the acceleration phases, deceleration was accompanied by drainage of subglacial water, evidenced by the filling of the glacier-dammed lake during the winters of 2014/15 and 2015/16. Lake drainage in July 2015 caused instantaneous deceleration over the whole glacier tongue, indicating that a sudden drainage of the subglacial water under a large part of the glacier tongue occurred with the lake outburst event.

Surging of Kyagar Glacier is the main driver of ice-dammed lake formation and GLOFs. The thickening of over 60 m at the glacier terminus during the surge caused potential GLOF size to increase almost 40-fold since early 2014, to ~~currently~~ over 70 million m^3 ~~.~~ at the end of summer 2016. The hazard potential of large GLOFs remains high in the next few years, potentially larger than the 2015 and 2016 GLOFs, but the actual magnitude depends on the timing of lake drainage. Remotely sensed data, in particular from TanDEM-X, ~~was~~ is essential to the observation of the surge phenomenon and the assessment of hazard formation. The remote sensing of the glacier should be continued to monitor lake formation and the evolution of the ice dam height.

Author contributions. VR wrote major parts of the paper, calculated velocity maps and analysed all data. SL developed the offset tracking algorithms and did the interferometric processing to obtain the DEMs. MH and CH initiated the study and contributed to discussion of the results throughout. IH provided feedback on a final version. The authors declare that they have no conflict of interest.

Acknowledgements. We would like to thank the German Space Agency DLR for providing TanDEM-X data through the proposal XTI_GLAC6780. We greatly appreciate the Landsat data available from the U.S. Geological Survey and the Copernicus Sentinel-1A and Sentinel-2 data from the European Space Agency ESA. Geo-

praevent AG provided access to data and images from the monitoring stations in China. We thank ETH Zurich for providing the funding for this study and M. Funk for ~~comments on an earlier version~~helpful comments on the manuscript.

References

Barrand, N. E. and Murray, T.: Multivariate Controls on the Incidence of Glacier Surging in the Karakoram Himalaya, Arctic, Antarctic and Alpine Research, 38, 489–498, 2006.

Björnsson, H.: Hydrological characteristics of the drainage system beneath a surging glacier, Nature, 395, 771–774, 1998.

Björnsson, H.: Understanding jokulhlaups; from the tale to theory, Journal of Glaciology, 56, 1002–1010, 2010.

Björnsson, H., Pálsson, F., Sigurdsson, O., and Flowers, G. E.: Surges of glaciers in Iceland, Annals of Glaciology, 36, 82–90, 2003.

Boulton, G. S. and Jones, A. S.: Stability of temperate ice caps and ice sheets resting on beds of deformable sediment, Journal of Glaciology, 24, 29–43, 1979.

Boulton, G. S. and Zatsepin, S.: Hydraulic impacts of glacier advance over a sediment bed, Journal of Glaciology, 52, 497–527, 2006.

Bourbigot, M., Johnsen, H., and Piantanida, R.: Sentinel-1 Product Specification, Tech. Rep. S1-RS-MDA-52-7441, European Space Agency, ESA Publications, ESTEC, Postbus 299, 2200 AG Noordwijk, The Netherlands, 2016.

Chen, Y., Xu, C., Chen, Y., Li, W., and Liu, J.: Response of glacial-lake outburst floods to climate change in the Yarkant River basin on northern slope of Karakoram Mountains, China, Quaternary International, 226, 75–81, 2010.

Clarke, G. K. C.: Length, width and slope influences on glacier surging, Journal of Glaciology, 37, 236–246, 1991.

Clarke, G. K. C., Collins, S. G., and Thompson, D. E.: Flow, thermal structure and subglacial conditions of a surge-type glacier, Canadian Journal of Earth Sciences, 21, 232–240, 1984.

Clarke, G. K. C., Schmock, J., Simon, C., Ommanney, L., and Collins, S. G.: Characteristics of Surge-Type Glaciers, Journal of Geophysical Research, 91, 7165–7180, 1986.

Copland, L., Sylvestre, T., Bishop, M. P., Shroder, J. F., Seong, Y. B., Owens, L. A., Bush, A., and Kamp, U.: Expanded and Recently Increased Glacier Surging in the Karakoram, Arctic, Antarctic and Apline Research, 43, 503–516, 2011.

Cuffey, K. M. and Paterson, W. S. B.: The Physics of Glaciers, Elsevier, 4 edn., 2010.

Dehecq, A., Millan, R., Berthier, E., Gourmelen, N., and Trouvé, E.: Elevation changes inferred from TanDEM-X data over the Mont-Blanc area: Impact of the X-band interferometric bias, IEEE Journal of Selected Topics in Applied Earth Observations and Remote Sensing, 22-24 July 2015, 2015.

Desio, A., Caporali, A., Gaettani, M., Gosso, G., Palmieri, F., Pognante, U., and Rampini, L.: Geodesy, Geophysics and Geology of the Upper Shaksgam Valley (North-East Karakoram) and South Sinkiang, Consiglio Nazionale delle Ricerche, 1991.

Dunse, T., Schnellenberger, T., Hagen, J. O., Kääb, A., Schuler, T. V., and Reijmer, C.: Glacier-surge mechanisms promoted by a hydro-thermodynamic feedback to summer melt, The Cryosphere, 9, 197–215, 2015.

Eisen, O., Harrison, W. D., Raymond, C. F., Echelmeyer, K. A., Bender, G. A., and Gorda, J. L. D.: Variegated Glacier, Alaska, USA: a century of surges, Journal of Glaciology, 51, 399–406, 2005.

Farr, T. G., Rosen, P. A., Caro, E., Crippen, R., Duren, R., Hensley, S., Kobrick, M., Paller, M., Rodirguez, E., Roth, L., Seal, D., Schaffer, S., Shimada, J., Umland, J., Werner, M., Oskin, M., Burbank, D., and Alsdorf, D.: The Shuttle Radar Topography Mission, Reviews of Geophysics, 45, 2007.

Fischer, G., Parrella, G., Papathanassiou, K., and Hajnsek, I.: Interpretation of Pol-InSAR Signatures from Glaciers and Ice Sheets at Different Frequencies, in: EUSAR 2016, 2016.

Fowler, A. C., Murray, T., and Ng, F. S. L.: Thermally controlled glacier surging, Journal of Glaciology, 47, 2001.

GAPHAZ, 2016: 17 July and 21 September 2016 glacier collapses in Tibet, online: http://gaphaz.org/, 2016.

Gardelle, J., Berthier, E., Arnaud, Y., and Kääb, A.: Region-wide glacier mass balances over the Pamir-Karakoram-Himalaya during 1999-2011, Cryosphere, 7, 1885–1886, 2013.

Goldstein, R. M. and Werner, C. L.: Radar interferogram filtering for geophysical applications, Geophysical Research Letters, 25, 4035–4038, 1998.

Goldstein, R. M., Zebker, H. A., and Werner, C. L.: Satellite radar interferometry - Two-dimensional phase unwrapping, Radio science, 23, 713–720, 1988.

Greve, R. and Blatter, H.: Dynamics of Ice Sheets and Glaciers, Springer Berlin Heidelberg, 1 edn., 2009.

Haemmig, C., Huss, M., Keusen, H., Hess, J., Wegmüller, U., Ao, Z., and Kulubayi, W.: Hazard assessment of glacial lake outburst floods from Kyagar glacier, Karakoram Mountains, China, Annals of Glaciology, 55, 34–44, doi:10.3189/2014AoG66A001., 2014.

Harrison, W. D. and Post, A. S.: How much do we really know about glacier surging?, Annals of Glaciology, 36, 2003.

Harrison, W. D., Osipova, G. B., Nosenko, G. A., Espizua, L., Kääb, A., Fischer, L., Huggel, C., Burns, P. A. C., Truffer, M., and Lai, A. W.: Chapter 13 Glacier Surges, in: Snow and Ice-Related Hazards, Risks and Disasters, Elsevier, 2014.

Heid, T. and Kääb, A.: Repeat optical satellite images reveal widespread and long term decrease in land-terminating glacier speeds, The Chryosphere, 6, 467–478, 2012.

Hewitt, H. and Liu, J.: Ice-dammed lakes and outburst floods, Karakoram Himalaya: historical perspectives on emerging threats, Physical Geography, 36, 528–551, doi:10.2747/0272-3646.31.6.528, 2010.

Hoinkes, H. C.: Surge of the Vernagtferner in the Ötztal Alps since 1599, Canadian Journal of Earth Sciences, 6, 853–861, doi:10.1139/e69-086, 1969.

Huss, M.: Density assumptions for converting geodetic glacier volume change to mass change, The Cryosphere, 7, 877–887, 2013.

Jiskoot, H. and Low, R. H.: Is seasonal timing of surge initiation or termination related to surge character and development?, AGU Fall Meeting Abstracts, pp. 503–516, 2011.

Jiskoot, H., Maurray, T., and Boyle, P.: Controls on the distribution of surge-type glaciers in Svalbard, Journal of Glaciology, 46, 412–422, 2000.

Kamb, B., Raymond, C. F., Harrison, W. D., Engelhardt, H., Echelmeyer, K. A., Humphrey, N., Brugman, M. M., and Pfeffer,

T.: Glacier Surge Mechanism: 1982-1983 Surge of the Variegated Glacier, Alaska, Science, 227, 469–479, 1985.

Kapnick, S. B., Delworth, T. L., Ashfaq, M., Malyshev, S., and Milly, P. C. D.: Snowfall less sensitive to warming in Karakoram than in Himalayas due to unique seasonal cycle, Nature Geoscience, 7, 834–840, 2014.

Krieger, G., Moreira, A., Fiedler, H., Hajnsek, I., Werner, M., Younis, M., and Zink, M.: TanDEM-X: A Sattelite Formation for High-Resolution SAR Interferomertry, IEEE Transactions on Geoscience and Remote Sensing, 45, 3317–3341, 2007.

Krieger, G., Zink, M., Bachmann, M., Bräutifam, B., Schulze, D., Martone, M., Rizzoli, P., Steinbrecher, U., Antony, J. A., Zan, F. D., Hajnsek, I., Papathanassiou, K., Kugler, K., and Cassola, F.: TanDEM-X: A radar interferometer with two formation-flying satellites, Acta Astronautica, 89, 83–98, 2013.

Leinss, S., Wiesmann, A., Lemmetyinen, J., and Hajnsek, I.: Snow Water Equivalent of Dry Snow Measured by Differential Interferometry, IEEE Journal of Selected Topics in Applied Earth Observations and Remote Sensing, 8, 3773–3790, 2015.

Luckman, A., Quincey, D., and Bevan, S.: The potential of satellite radar interferometry and feature tracking for monitoring flow rates of Himalayan glaciers, Remote sensing of Environment, 111, 172–181, 2007.

Mason, K.: Exploration of the Shaksgam Valley and Aghil Ranges, 1926, Survey of India, 1928.

Mayer, C., Fowler, A. C., Lambrecht, A., and Schnarrer, K.: A surge of North Gasherbrun Glacier, Karakoram, China?, Journal of Glaciology, 57, 904 – 916, 2011.

Meier, M. F. and Post, A.: What are glacier surges?, Canadian Journal of Earth Sciences, 6, 807–817, 1969.

Murray, T., Stuart, G. W., Miller, P. J., Woodward, J., Smith, A. M., Porter, P. R., and Jiskoot, H.: Glacier surge propagation by thermal evolution at the bed, Journal of Geophysical Research, 105, 134 991 – 13 507, 2000.

Nagler, T. and Rott, H.: SAR tools for snowmelt modelling in the project HydAlp, in: Geoscience and Remote Sensing Symposium Proceedings, 1998. IGARSS '98. 1998 IEEE International, pp. 1521–1523 vol.3, 1998.

Nagler, T., Rott, H., Ripper, E., Bippus, G., and Hetzenecker, M.: Advancements for Snowmelt Monitoring by Means of Sentinel-1 SAR, Remote Sensing, 8, 2016.

Ng, F., Liu, S., Mavlyudov, B., and Wang, Y.: Cliamtic control on the peak discharge of glacier outburst floods, Geophysical Research Letters, 34, 2007.

Quincey, D. J. and Luckman, A.: Brief Communication: On the magnitude and frequency of Khurdopin glacier surge events, The Cryosphere, 8, 571–574, 2014.

Quincey, D. J., Braun, M., Glasser, N. F., Bishop, M. P., and Luckman, A.: Karakoram glacier surge dynamics, Geophysical Research Letters, 38, 2011.

Quincey, D. J., Glasser, N. F., Cook, S. J., and Luckman, A.: Heterogeneity in Karakoram glacier surges, Journal of Geophysical Research: Earth Science, 120, 1288–1300, 2015.

Randolph Glacier Inventory Version 5.0: Global Land Ice Measurements from Space, Boulder Colorado, USA. Digital Media., Tech. rep., http://www.glims.org/RGI/index.html, 2015.

Raymond, C. F.: How Do Glaciers Surge?, Journal of Geophysical Research, 92, 9121–9134, 1987.

Rignot, E., Echelmeyer, K., and Krabill, W.: Penetration depth of interferometric synthetic-aperture radar signals in snow and ice, Geophysical Research Letters, 28, 3501–3504, 2001.

Searle, M. P. and Phillips, R. J.: Relationships between right-lateral shear along the Karakoram Fault and metamorphism, magmatism, exhumation and uplift: evidence from the K2-Gashebrum-Pangong ranges, north Pakistan and Ladakh, Journal of the Geological Society, London, 164, 439–450, 2007.

Sevestre, H. and Benn, D. I.: Climatic and geometric controls on the global distribution of surge-type glaciers: implications for a unifying model of surging, Journal of Glaciology, 61, 646–659, 2015.

Sevestre, H., Benn, D. I., Hulton, N. R. J., and Baelum, K.: Thermal structure of Svalbard glaciers and implications for thermal switch models of glacier surging, Journal of Geophysical Research, 120, 2220–2236, 2015.

Small, D.: SAR backscatter multitemporal compositing via local resolution weighting, in: Geoscience and Remote Sensing Symposium (IGARSS), 2012 IEEE International, pp. 4521–4524, 2012.

Strozzi, T., Luckman, A., Murray, T., Wegmüller, U., and Werner, C. L.: Glacier Motion Estimation Using SAR Offset-Tracking Procedures, IEEE Transactions on Geoscience and Remote Sensing, 40, 2384–2390, 2002.

Truffer, M., Harrison, W. D., and Echelmeyer, K. A.: Glacier motion dominated by processes deep in underlying till, Journal of Glaciology, 46, 213–221, 2000.

Vaughan, D. G.: Recent Trends in Melting Conditions on the Antarctic Peninsula and Their Implications for Ice-sheet Mass Balance and Sea Level, Arctic, Antarctic and Alpine Research, 38, 147–152, 2006.

Weertman, J.: Water lubrication mechanism of glacier surges, Canadian Journal of Earth Sciences, 6, 929–942, 1969.

Yasuda, T. and Furuya, M.: Dynamics of surge-type glaciers in West Kunlun Shan, Northwestern Tibet, Journal of Geophysical Research: Earth Surface, 120, 2015.

Zebker, H. A. and Villasenor, J.: Decorrelation in interferometric radar echos, Geoscience and Remote Sensing, IEEE, 30, 950–959, 1992.

Zebker, H. A. and Yanping, L.: Phase unwrapping algorithms for radar interferometry: residue-cut, least-squares, and synthesis algorithms, Journal of the Optical Society of America, 15, 586–598, 1998.

Zhang, X.: Investigation of glacier bursts of the Yarkant River in Xinjiang, China, Annals of Glaciology, 16, 135–139, 1992.

Zitova, B. and Flusser, F.: Image registration methods: a survey, Image and Vision Computing, 21, 977-1000, 2003.